Energy & Environmental Science

Mining Bitcoins with Carbon Capture and Renewable Energy for Carbon Neutrality Across States in the USA

SCHOLARONE™
Manuscripts

Title: Mining Bitcoins with Carbon Capture and Renewable Energy for Carbon Neutrality Across States in the USA

Manuscript ID: EE-ANA-12-2021-003804.R2

Broader context:

Bitcoin mining's thirst for energy consumption and associated carbon emissions have raised concerns across the globe. The recent bitcoin boom led to a significant increase in electricity demand and carbon emissions. A few countries, such as China, Russia, and Iran, banned bitcoin mining to prevent grid imbalances and environmental damages. As a result, miners are moving to the U.S. for cheaper electricity and more mining freedom. However, concerns remain regarding economic and environmental integrity. This study, therefore, examines bitcoin's economic and environmental standing across the U.S. states for potential mining sites. Sustainable mining is achievable via initiatives, such as carbon capture and renewable-powered mining farms. States with a large share of renewable energy in the electrical grid and lower electricity prices can potentially mitigate environmental damages. This study also compares the break-even selling prices of bitcoin to determine potential profit margins for mining sites in different states. The study's findings provide a deep understanding of the policy implications of balancing economic development and environmental protection. Incentives for carbon capture and eco-friendly mining will benefit relevant stakeholders if policymakers and bitcoin investors take appropriate action.

PAPER

Mining Bitcoins with Carbon Capture and Renewable Energy for Carbon Neutrality Across States in the USA

Haider Niaz,[a,b] Mohammad H. Shams,[c] Jay. J Liu,*[a,c] and Fengqi You*[b]

Bitcoin mining requires a significant amount of electricity to validate blocks, increasing greenhouse gas emissions. Therefore, major countries such as China, Iran, Russia, Turkey, and Vietnam are banning bitcoin mining to avoid grid imbalances, power failures, and environmental issues. To alleviate these concerns, we conducted a techno-economic analysis of 50 states and a federal district (Washington D.C.) in the US in terms of the feasibility of bitcoin mining using carbon capture and renewable energy. We analyzed the profitability of bitcoin mining in the US states using grid and renewable power resources along with high-temperature and low temperature direct air capture technologies for CO_2 capture and storage and methanol as a product. From both economic and environmental perspectives, we evaluated the net CO_2 emission for each state to determine its competitive advantages. Overall, this work offers a holistic overview of where bitcoin mining can be economically viable across US states. Additionally, it provides insights into achieving environmentally friendly cryptocurrency mining regulations based on carbon capture and renewable energy and gauging the costs of bitcoin mining powered by the grid and high renewable penetration across the US states while pursuing carbon neutrality.

Introduction

Currently, the use of fossil fuels is inevitable due to the lack of sustainable resources to meet the energy demand, leading to substantial carbon emissions. Although renewables also participate in electricity generation, their fluctuating nature and high capital expenses make them uncompetitive to provide affordable electricity. Among grid electricity consumers, besides industrial, commercial, and residential users, new consumers have recently emerged, i.e., crypto miners, raising concerns over both the adequacy of power grids and environmental aspects. Among various cryptocurrencies, bitcoin has caused the highest energy consumption and often resulted in grid failures due to electricity shortages [1]. According to the Cambridge bitcoin electricity consumption index, bitcoin mining consumes an estimated 111.63 TWh of electricity yearly with estimated theoretical lower and upper bounds of 40.54 and 418.46 TWh, respectively[2]. This estimated power consumption accounts for 2.91% of the annual electricity consumption of the US and corresponds to the electricity demands of some countries, such as Poland, Sweden, Finland, and Norway [3]. In addition, bitcoin mining generates additional

CO_2 emissions associated with the vast electricity consumption, accounting for 90.76 million tons of CO_2 emission annually [4]. As the world is already scrambling to meet the goals of the Paris agreement, with the emergence of new grid consumers, the devastating impacts of cryptocurrency use are yet to be seen on the progress in achieving these goals [5]. On September 14, 2021, China started a crackdown on crypto miners and banned all cryptocurrency transactions and mining activities. As a result, miners started to move to other cryptocurrency-friendly countries, such as Serbia, and predominantly to New York and Texas in the US, accounting for 19.9% and 14% of bitcoin's hash rate share within the US, respectively [6].

Nevertheless, it is unclear whether mining in these states will be viable for the economy and the environment. Therefore, the main goal of this study was to determine the best US states for investment in bitcoin mining farms by considering technical, economic, and environmental aspects.

Blockchain consists of chronologically and cryptographically connected blocks that are a set of transaction records validated and approved by participating miners on the blockchain network [7]. The network security is ensured by connecting each block in the chain pattern with the digital signature of the previous block. Any change in the block requires validation, which follows a series of steps and a protocol called the consensus mechanism. The commonly known blockchain consensus mechanisms include Proof of Stake (PoS) and Proof of Work (PoW) [8]. Bitcoin follows a PoW mechanism that validates transactions and maintains a highly secure blockchain. However, this mechanism has been criticized for not utilizing computer resources efficiently, which comes with additional power consumption [9]. Compared to PoS, PoW has proven to be

[a.] Department of Chemical Engineering, Pukyong National University, Busan 48513, Republic of Korea.

[b.] Smith School of Chemical and Biomolecular Engineering, Cornell University, Ithaca, New York 14853, United States of America

[c.] Institute of Cleaner Production Technology, Pukyong National University, Busan 48547, Republic of Korea

† Footnotes relating to the title and/or authors should appear here.

Electronic Supplementary Information (ESI) available: [details of any supplementary information available should be included here]. See DOI: 10.1039/x0xx00000x

more reliable so far in maintaining the security of a distributed public network [10]. Moreover, PoW is the only consensus mechanism that has been proven at scale, making it better than PoS and thus more effective [11].

In 2008, Satoshi founded bitcoin, a digital currency that relies on a decentralized system, where participants provide computing power to validate transactions and secure network integrity by solving mathematical problems. Each verified transaction is incentivized with a digital currency known as bitcoin [12]. The power needed to mine a bitcoin was initially low. However, in 2018, the computational power required for bitcoin mining increased four-fold, correspondingly increasing power consumption. Besides, the profitability of bitcoin mining highly depends on mining equipment and electricity affordability in the region. So, the location and the miner must be chosen carefully. With the increase in the bitcoin price, investors started investing in their own mining farms, while individual miners joined mining pools and supplied computational power to solve blocks to be added to the blockchain to mine bitcoins [13]. All these miners consumed excessive power for their mining equipment and needed auxiliaries to provide cooling and ensure mining efficiency. Higher power consumption from the grid raised concerns as associated carbon emissions also increased. In this context, renewable energy can be a sustainable option to power bitcoin farms. However, their fluctuating nature makes them a less reliable resource unless coupled with energy storage options such as battery energy storage systems (BESS) or energy in the form of hydrogen [14]. It is largely unknown whether investing in renewable infrastructure would be a plausible solution, considering the fluctuating bitcoin price and the intermittent nature of renewable energy. Relevant literature on economic and environmental assessments of using grid and renewable electricity for bitcoin farming is relatively scarce, making it hard for investors and policymakers to develop relevant solutions [15]. Little work has been conducted on bitcoin investments, making it difficult to analyze its potential in the long term. Orcutt discussed the bitcoin mining rush in Texas, US using wind farms and suggested installing 100 MW of electricity specifically for bitcoin mining [16]. Chinese mining chip maker Bitman migrated to start a 50 MW facility in Rockdale, Texas, with an investment of around USD 500 million[17]. A German firm, Northern data, also plans to invest in Rockdale, Texas to build the world's largest bitcoin mining facility[16]. Recently, Northern Data acquired the bitcoin mining company Bitfield N.V., becoming a global player with around 33,000 latest generations of application-specific integrated circuits (ASICs) [18]. However, a considerable gap lies in the assessment of other states as potential bitcoin mining sites. Huge investments will likely follow, including that of the financial firm Square Inc. [19]. From the operational and economic perspectives, Bastian-Pinto et al. discussed balancing renewable investments in wind farms and bitcoin mining by optimally selecting outputs (electricity and bitcoin mining) that can maximize return and reduce economic risks [20]. Andoni et al. reviewed blockchains in the energy sector and emphasized the benefits of blockchain for energy system operation, market, and consumers [21]. They further discussed how bitcoin mining could create balance in the energy market and act as shock absorbers in the volatile energy price market. Bitcoin mining can also serve as a balancing element when the renewable supply surges to accommodate any surplus generation from renewable power, hence reducing yearly curtailments[22]. However, the environmental impacts of grid-powered bitcoin mining outweigh its economic advantages.

Regardless of the benefits of the bitcoin economy, its environmental impacts will be seen in the long term [23]. Stoll et al. examined the carbon footprint of bitcoin [13]. They reported an estimated 45.8 TWh with annual carbon emissions in the range of 22–22.9 Mt CO_2 originating from bitcoin mining for the year 2018 alone, equivalent to emissions produced by countries such as Jordan and Sri Lanka. Although the fate of bitcoin is hard to predict, Mora et al. suggested that bitcoin will increase the electricity demand, which can cause a global temperature increase of above 2°C in just a few decades [24]. Lars et al. also supported this prediction [25]. In addition, non-functional and scrapped mining equipment added an annual 30.7 metric kilotons of e-waste as of May 2021 [26]. Renewable-powered bitcoin mining farms can be interesting to investigate as they can provide tangible support to balance energy supply and demand and reduce carbon emissions to a great extent. However, due to the massive investments needed for renewable infrastructure, comprehensive analysis in terms of cost benefits and environmental sustainability is required [19].

A rigorous study is needed to explore the hidden economic and environmental impacts of bitcoin mining by the grid and renewable resources. Even though miners are rushing to Texas for cheaper electricity costs, the resulting environmental damages are still unknown. Besides, other US states may also provide competitive advantages over Texas. Therefore, we analyzed eight different scenarios with grid-only-powered (GOP) and high renewable penetration-powered (HRPP) bitcoin mining farms considering multiple factors that define each scenario's actual economic and environmental standings for the US states. The tackled research gaps have been highlighted in the following study contributions:

I.   This study evaluated US states as potential candidates for GOP and HRPP bitcoin mining via carbon capture and utilization initiatives.

II. The carbon footprint was estimated for each state. Furthermore, carbon emissions were calculated using the grid electricity consumption based on the non-renewable share for respective states.

III. The electricity price, wind speed, solar irradiation, and state-wise solar capacity factor were collected for one year to determine the optimal grid and renewable share for a bitcoin mining farm.

IV. The direct air capture (DAC) and methanol production plants were then sized to capture the emissions. Based on their respective power consumption, the optimal numbers of electrolyzers (ELE), fuel cells (FCs), heat pumps (HP), BESS, hydrogen tanks (HTANKs), and green hydrogen needed were evaluated.

2 | *Energy Environ. Sci.* 2021, **00**, 1-3

This journal is © The Royal Society of Chemistry 20xx
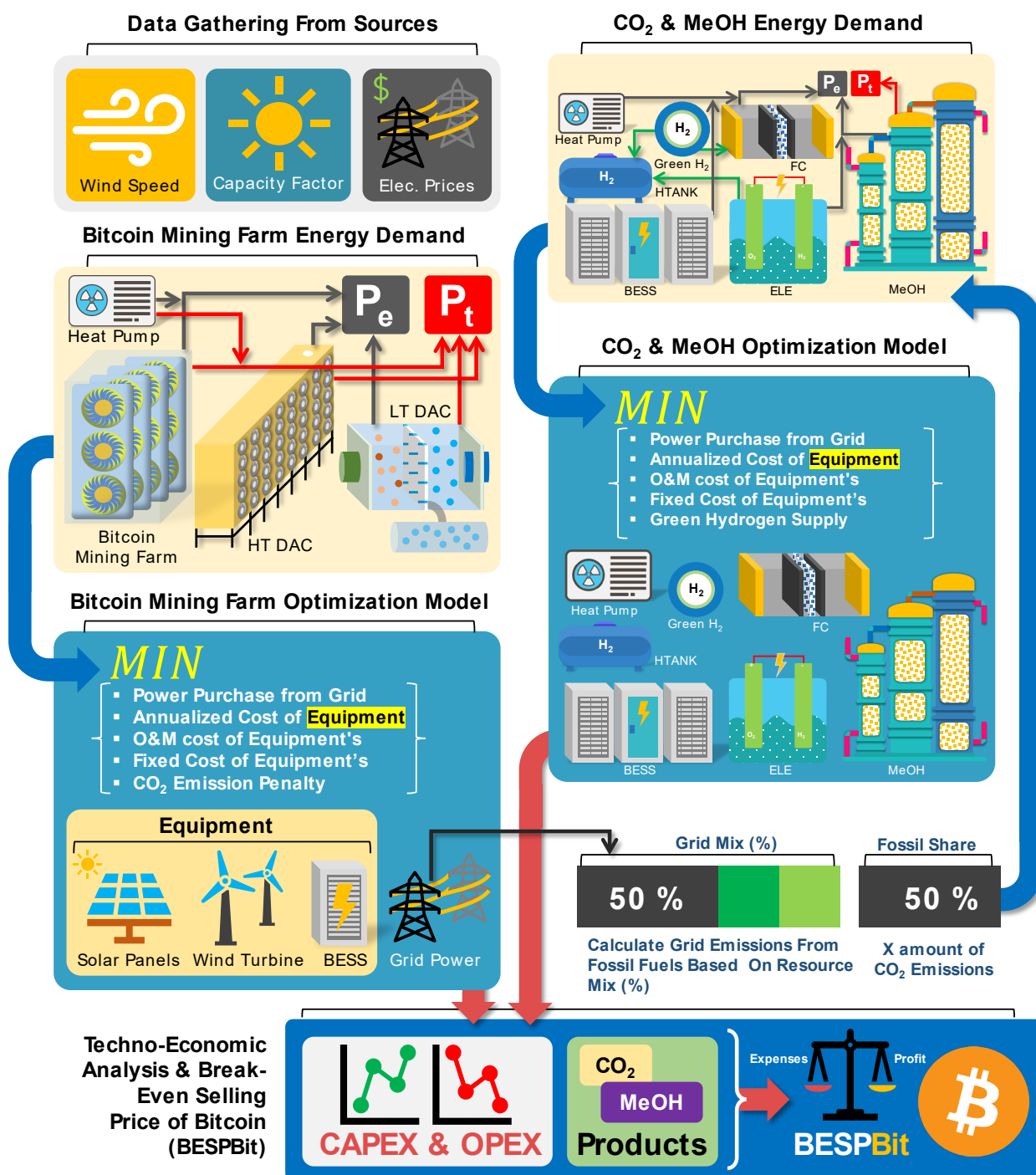
Figure 1. Proposed framework for evaluating the BESPBit for various US states.

V. These results were then used in the comprehensive economic analysis to evaluate the break-even selling price of bitcoin (BESPBit).

Overall, this study will help investors and policymakers make informed decisions about cryptocurrency mining, paving the way for its sustainable implementation in the future.

The rest of the paper is organized as follows. In Section 2, preliminaries are described. Section 3 describes the framework of the study. The case study and system description are elaborated in Section 4. Section 5 presents the results and discussion. Finally, the paper is concluded in Section 6.

Preliminaries

Bitcoin mining farms and miners

Crypto mining farms are technically data centers equipped with devices with high computational power designed to solve complex mathematical problems to mine a cryptocurrency as

This journal is © The Royal Society of Chemistry 20xx

Energy Environ. Sci. 2021, **00**, 1-3 | **3**

an incentive. Bitcoins can be mined in diverse ways: individually with small computational power, at a large scale with thousands of mining equipment and hash power, or by joining a mining pool where individuals sign up and supply their mining power and, as a result, earn their relative share. The devices that mine cryptocurrencies are called miners.

DAC model

DAC systems are the most developed and commercially available technology to capture CO_2 in the air [27]. Besides their commercial advancement, negative emissions can be achieved by CO_2 storage and mineralization. Furthermore, captured CO_2 can be used as a feedstock for carbon-based fuels, other value-added chemicals, and building materials [28]. Thus, the DAC approach was adopted for CO_2 capture. It can either be a high-temperature aqueous solution (HT-DAC) or a low-temperature solid sorbent (LT-DAC) system. As the name suggests, HT-DAC is an energy-intensive process that captures CO_2 in the air when the air meets a solvent in the absorption column under ambient conditions. The solution with captured CO_2 goes through a regeneration cycle in which depleted CO_2 air leaves the column, and the solvent then undergoes HT processing to recover the solvent and extract CO_2[29]. Similarly, LT-DAC uses low temperature and a solid sorbent to absorb CO_2, which releases the captured CO_2 from the air upon mild heating. Both technologies have their advantages and shortcomings: HT-DAC can handle larger quantities, whereas LT-DAC can handle one-third of the capacity of HT-DAC [29].

Methanol production facility

The methanol facility utilizes CO_2 and H_2 as raw materials to produce MeOH. MeOH was chosen as a pathway due to multiple reasons, which can be listed as follows:

    I.   MeOH is an attractive fuel in emerging economies as a liquid fuel to replace conventional carbon-intensive energy sources. [30,31]

    II.   Formaldehyde, the main derivative of MeOH, accounts for 31% of the world's MeOH demand. Other uses include biodiesel, gasoline blending, and dimethyl ether. The high global MeOH demand drives its production growth, which is expected to increase at an average rate of 5% in the next five years and as a fuel at a rate of 6.5%[30]. Besides, MeOH is a versatile chemical compound that serves as a fuel and hydrogen energy carrier and is also a base chemical for the chemical and petrochemical industry [32]. In addition, the global demand for MeOH is increasing due to its role in monomeric olefin production, such as ethylene and propylene, the bases of the plastic industry.

    III.   Lastly, MeOH is the best option due to its technological maturity and compatibility with the current fuel infrastructure, production cost, and public acceptance[32].

Therefore, the MeOH pathway was explored for the GOP and HRPP scenarios owing to its rising global demand.

Framework of the study

The methodology adopted in this study to evaluate the BESPBit across various US states is described in the following steps.

Step 1: As shown in Figure 1, the process starts with collecting the data for wind speed, solar irradiation, and average hourly monthly price for grid electricity. Furthermore, for the grid-based electricity, the percentage of resource mix (%), i.e., fossil or renewables was also collected for individual US states to find out the actual fossil-based contribution for mining bitcoins. By using the contribution fraction of the consumed respective fossil resource, i.e., coal, natural gas, oil, etc., the equivalent amount of CO_2 emitted was calculated to size the system needed for the downstream process. The amount of CO_2 emissions from each of the respective fossil resources (per MW of produced power) was obtained from the US Energy Information Administration (EIA) and other sources[31,33,34]. The DAC and MeOH plants were introduced to make bitcoin mining environmentally sustainable despite their vast energy consumption.

Step 2: Two scenarios were considered to power the bitcoin mining farm: GOP and HRPP scenarios. Only wind and solar resources were considered for renewable sources due to a lack of data resources for other renewable resources in other states. The time resolution for the data used was one hour for 1 year, i.e., 8760 points. An optimization model was run for the GOP scenario to evaluate the optimal number of solar panels, wind turbines, and grid power needed to run the mining farm and the cooling system. The objective function was set to minimize the annual cost while also considering the penalty of CO_2 emissions when utilizing the grid-based power. By using the optimal grid share value, the equivalent amount of CO_2 emissions was evaluated and used as a basis for the DAC plant.

Step 3: Based on the amount of CO_2 emissions calculated in Step 2, the size of the DAC plant and its electrical and thermal requirements were evaluated. Two different DAC plants were considered: HT-DAC and LT-DAC plants. Both vary in cost, energy requirements, and their respective capturing capacities. Furthermore, two different routes were considered: CO_2 capture and storage and MeOH as a product. Later, the amount of grid power needed was evaluated for the GOP scenario to satisfy the electrical and thermal demand. In contrast, for the HRPP case scenario for CO_2 capture and storage, and MeOH as a product, the optimal numbers of FCs, ELEs, HPs, BESS, and HTANKs, and green hydrogen supply needed to meet the energy demands were evaluated using an annual cost minimization objective function, similar to the one used for the mining farm but with additional equipment. Similarly, the optimal configuration was re-evaluated for MeOH as a product for all states.

Step 4: Finally, using the optimal numbers evaluated from the optimization model for meeting mining farm energy demands and DAC and MeOH optimization models, the total number of equipment and their respective CAPEX and OPEX were recalculated. A comprehensive economic analysis was performed to determine the BESPBit for US states for each scenario.

Step 5: The results were then compared for each scenario's most and least favorable US states, respectively. Furthermore,

4 | *Energy Environ. Sci.* 2021, **00**, 1-3

This journal is © The Royal Society of Chemistry 20xx

all cases were collectively compared, and recommendations and conclusions were drawn for each scenario's best and worst states for bitcoin mining investments.

Mathematical Formulation

Objective function

In the proposed formulations, the total annual cost (TAC) of the system is minimized via the decision variables, including the number of units of each equipment type (i.e., N^{PV}, N^{WT}, N^{ELE}, N^{FC}, N^{HP}, N^{BESS}, and N^{HTANK}), binary variables for on/off of the BESS, i.e., u_t^1, u_t^2., electricity delivered to the equipment (PE^{ELE}, PE^{HP}, and PE^{BESS}), electricity purchased from the grid (PE^{GRID}), green hydrogen (H^{REN}), and hydrogen delivered to the FC and HTANK (H^{FC} and H^{HTANK}, respectively). The results from the optimization model will serve as a basis for the economic analysis.

The formulated optimization problem used for calculating the optimal numbers of solar panels and wind turbines and grid electricity required for bitcoin mining for all scenarios is shown in Eqs. (1) and (2), which include annualized CAPEX, fixed and variable operations, and maintenance costs. It also considered the penalty for the use of grid electricity. The optimization problem for DAC and methanol plants can be seen in Eq. (1b). No grid electricity was considered for DAC and methanol plants; therefore, no CO_2 emissions penalty costs were included in the objective function. The overall problem was formulated as a MILP problem and solved using the CPLEX solver in GAMS [35].

$$\sum_{t=1}^{T}\{PE_t^{GRID} \cdot C_t^{GRID} + ANC^{PV} + ANC^{WT} + ANC^{HP} + ANC^{BESS} + O\&M_t^{PV} + O\&M_t^{WT} + O\&M_t^{HP} + O\&M_t^{BESS} + FOC^{PV} + FOC^{WT} + FOC^{HP} + FOC^{BESS} + PE_t^{GRID} \cdot PC_{PE}^{CO2}\} \quad (1)$$

$$\sum_{t=1}^{T}\{H_t^{REN} \cdot C_H^{REN} + ANC^{PV} + ANC^{WT} + ANC^{ELE} + ANC^{FC} + ANC^{HP} + ANC^{BESS} + ANC^{HT} + O\&M_t^{PV} + O\&M_t^{WT} + O\&M_t^{ELE} + O\&M_t^{FC} + O\&M_t^{HP} + O\&M_t^{BESS} + O\&M_t^{HT} + FOC^{PV} + FOC^{WT} + FOC^{AWE} + FOC^{FC} + FOC^{HP} + FOC^{BESS} + FOC^{HT}\} \quad (2)$$

Constraints

The overall electricity, cooling, and hydrogen balances can be represented as PE_t^{LOAD}, PC_t^{LOAD}, and H_t^{LOAD}, respectively. For the bitcoin scenario, only the grid, PV, WT, and BESS were considered, whereas, for the DAC and methanol plant, all equipment were considered with the addition of green hydrogen supply, except for the grid electricity. Therefore, the following constraints accounted for general scenarios. For respective case scenarios, equipment not considered was taken as zero.

$$PE_t^{LOAD} - PE_t^{GRID} + PE_t^{BESS.P} \cdot \eta^{BESS.P} - PE_t^{BESS.M} \cdot \eta^{BESS.M} + PE_t^{HP} + PE_t^{ELE} - PE_t^{FC} = PE_t^{WIND} + PE_t^{SOLAR} \quad (3)$$

$$PC_t^{LOAD} = PE_t^{HP} \cdot COP^{HP} \quad (4)$$

$$H_t^{LOAD} = H_t^{ELE} + H_t^{REN} - H_t^{HT.P} \cdot \eta^{HT.P} + H_t^{HT.M} \cdot \eta^{HT.M} - H_t^{FC} \quad (5)$$

The upper (*MAX*) and lower (*MIN*) penetration limits of electricity (*PE*) from the electrical power grid were represented as, respectively,

$$PE_{MIN}^{GRID} \le PE_t^{GRID} \le PE_{MAX}^{GRID} \quad (6)$$

These parameters (PE_{MIN}^{GRID}, and PE_{MAX}^{GRID}) representing the electrical grid constraints are defined later in the section. The upper and lower limits of green hydrogen, H_{MIN}^{REN} and H_{MAX}^{REN}, respectively, were represented as

$$H_{MIN}^{REN} \le H_t^{REN} \le H_{MAX}^{REN} \quad (7)$$

The main units include the PVs, WTs, ELEs, FCs, HPs, HTANKs, and BESS. The governing operation equations and sizing constraints are discussed below [36].

Power generated by wind turbines is dependent on the incident wind speed. Furthermore, the wind turbine characteristics are the key players in power generation including the cut-in speed and the cut-out speed (m/s). A piecewise linear equation was used to calculate the wind turbine output power as a function of incident wind speed, as shown in the equation below [37]:

$$PE_t^{WT} = \begin{cases} PE_r^{WT}, v_r < v_t^s < v_{cout} \\ PE_r^{WT} \cdot \frac{v_t^s - v_{cin}}{v_r - v_{cin}}, v_{cin} < v_t^s < v_r \\ 0, otherwise \end{cases} \quad (8)$$

PE_t^{WT} is the wind power output (in MW) at time t. PE_r^{WT} is the rated output of the wind turbine (in MW). v_r, v_{cin}, v_{cout} are the rated wind speed and the cut-in and cut-out wind speeds, respectively (in m/s). v_t^s is the wind speed at any given location at time t.

A PV system converts solar radiation into power. It is a function of incident radiation (W/m²), the efficiency of the solar panel, and the surface area of collector panels. It can be represented as a linear function as shown below [37]:

$$PE_t^{PV} = \eta^{PV} \cdot r_t^s \cdot S^{PV} \quad (9)$$

PE_t^{PV} is the output PV power, η^{PV} is the solar panel efficiency, which is considered as the capacity factor for a given location, r_t^s (W/m²) is the incident solar irradiation, and S^{PV} is the panel surface area (m²).

The amount of hydrogen produced in an ELE at any given hour (H_t^{ELE}) can be calculated using the relationship shown in Eq. (10) [14], where η^{ELE} represents the efficiency of the ELE, PE_t^{ELE} represents the electricity input to the ELE, and LHV_H represents the lower heating value of hydrogen.

$$H_t^{ELE} = \frac{\eta^{ELE} \cdot PE_t^{ELE}}{LHV_H} \quad (10)$$

The electricity provided to the ELEs is constrained by the number of ELEs (N^{ELE}) multiplied by the minimum and maximum amount of electricity provided to a single ELE, as shown in Eq. (11):

$$N^{ELE} \cdot PE_{MIN}^{ELE} \leq PE_t^{ELE} \leq N^{ELE} \cdot PE_{MAX}^{ELE} \qquad (11)$$

Similarly, in the governing equation of the FCs [Eq. (12)], PE_t^{FC} represents the electrical power output by the FC, H_t^{FC} represents the hydrogen supplied to the FC, and η^{FC} represents the fuel cell efficiency. The electricity output by the FC is constrained by the number of fuel cells (N^{FC}) multiplied by the minimum and maximum electricity outputs of a single FC, as shown in Eq. (13).

$$PE_t^{FC} = H_t^{FC} \cdot \eta^{FC} \cdot LHV_H \qquad (12)$$

$$N^{FC} \cdot PE_{MIN}^{FC} \leq PE_t^{FC} \leq N^{FC} \cdot PE_{MAX}^{FC} \qquad (13)$$

Likewise, HPs are governed by Eq. (14); the electricity supplied to the HPs is constrained by the number of heat pumps (N^{HP}) multiplied by the minimum and maximum electricity requirements of a single HP.

$$N^{HP} \cdot PE_{MIN}^{HP} \leq PE_t^{HP} \leq N^{HP} \cdot PE_{MAX}^{HP} \qquad (14)$$

The equations governing the BESS and HTANKs operate similarly. The BESS store electricity, and the HTANKs store hydrogen. The BESS cannot be charging and discharging at the same time, whereas this limitation does not apply to the HTANK. The state of charge (SOC) and state of hydrogen (SOH) at any given hour can be respectively represented as

$$SOC_t^{BESS} = SOC_{t-1}^{BESS} + PE_t^{BESS.P} \cdot \eta^{BESS.P} - PE_t^{BESS.M} \cdot \eta^{BESS.M} \qquad (15)$$

$$SOH_t^{HTANK} = SOH_{t-1}^{HTANK} + H_t^{HTANK.P} \cdot \eta^{HTANK.P} - H_t^{HTANK.M} \cdot \eta^{HTANK.M} \qquad (16)$$

where $PE_t^{BESS.P}$ and $PE_t^{BESS.M}$ represent the electricity charged to and discharged from the battery, respectively, and $\eta^{BESS.P}$ and $\eta^{BESS.M}$ represent the respective charging and discharging efficiencies. Similarly, $H_t^{HTANK.P}$ and $H_t^{HTANK.M}$ represent the hydrogen charged to and discharged from the HTANK, respectively, and $\eta^{HTANK.P}$ and $\eta^{HTANK.M}$ represent the respective charging and discharging efficiencies. The upper and lower electricity and hydrogen charging and discharging constraints are represented in Eq. (15) and Eq. (16), where N^{BESS} represents the number of BESS units, N^{HTANK} represents the number of HTANKs, SOC_{MIN}^{BESS} and SOC_{MAX}^{BESS} represent the minimum and maximum SOC of the BESS, respectively, and SOH_{MIN}^{HTANK} and SOH_{MAX}^{HTANK} represent the minimum and maximum SOH of the HTANKs, respectively.

$$N^{BESS} \cdot SOC_{MIN}^{BESS} \leq SOC_t^{BESS} \leq N^{BESS} \cdot SOC_{MAX}^{BESS} \qquad (17)$$

$$N^{HT} \cdot SOH_{MIN}^{HT} \leq SOH_t^{HT} \leq N^{HT} \cdot SOH_{MAX}^{HT} \qquad (18)$$

The following constraints were introduced to avoid charging and discharging the BESS units at the same time:

$$PE_t^{BESS.P} \leq u_t^1 \cdot PE_{MAX}^{BESS.P} \qquad (19)$$

$$PE_t^{BESS.M} \leq u_t^2 \cdot PE_{MAX}^{BESS.M} \qquad (20)$$

$$u_t^1 + u_t^2 \leq 1 \qquad (21)$$

where $PE_t^{BESS.P}$ and $PE_t^{BESS.M}$ represent the electricity charged to and discharged from the BESS, respectively, u_t^1 and u_t^2 represent the respective binary variables for charging and discharging the BESS, and $PE_{MAX}^{BESS.P}$ and $PE_{MAX}^{BESS.M}$ are the parameters representing the maximum electric charge and discharge, respectively.

The annualized system cost (ANC) was considered to represent system costs as it comprises the annualized capital cost, annualized replacement costs, and annualized maintenance costs [38]. The annualized cost of each equipment piece was calculated by multiplying the respective capital recovery factor (CRF) by the cost of the equipment:

$$CRF = \frac{IR \cdot (1+IR)^{NY}}{(1+IR)^{NY} - 1} \qquad (22)$$

The equipment and their respective replacement costs were annualized using Eq. (22) and are shown below in Eqs. (23)–(26). The degradation cost of the BESS ($C_t^{DEG.BESS}$) over time is shown in Eq. (26) [39].

$$ANC^X = \left(N^X \cdot C^X + RC^X \cdot \left(\frac{NY}{NY^X} \right) \right) \cdot CRF \qquad (23)$$

$$ANC^{ELE} = \left(N^{ELE} \cdot C^{ELE} + RC^{ELE} \cdot \left(\frac{NY}{NY^{ELE}} \right) \right) \cdot CRF \qquad (24)$$

$$ANC^{BESS} = \left(N^{BESS} \cdot C^{BESS} + RC^{BESS} \cdot \left(\frac{NY}{NY^{BESS}} \right) \right) \cdot CRF + \sum_{t=1}^{T_f} C_t^{DEG.BESS} \qquad (25)$$

$$C_t^{DEG.BESS} = C^{DEG} \cdot \left(PE_t^{BESS.P} \cdot \eta^{BESS.P} + \frac{PE_t^{BESS.M}}{\eta^{BESS.M}} \right) \qquad (26)$$

Here, NY represents the facility lifetime; the superscripts PV, WT, ELE, FC, HP, BESS, and HTANK represent the ANC or lifetime of their respective equipment. The lifetime of each equipment was used to calculate the number of replacements needed for each system and the associated replacement costs.

The operating costs for each of the PV, WT, ELE, FC, CCHP, HP, BESS, and HTANK subsystems were broken down to better understand the costs during operation, as detailed in Eqs.(27)–(29), respectively.

$$O\&M_t^X = OMC^X \cdot PE_t^X \qquad (27)$$

$$O\&M_t^{ELE} = \left(f_w \cdot \pi_w + f_{KOH} \cdot \pi_{KOH} + f_{N_2} \cdot \pi_{N_2} + f_S \cdot \pi_S \right) \cdot H_t^{ELE} \qquad (28)$$

$$O\&M_t^{BESS} = OMC^{BESS} \cdot PE_t^{BESS.P} \qquad (29)$$

where $O\&M$ represents the operation and maintenance cost of the respective equipment at any given hour, and OMC represents the summed operational and maintenance cost of

Table 1. Parameters for DAC and MeOH electrical and thermal energy requirements.

Process Section	Electrical/Heating Demand	Units	Reference
HT DAC	0.33/1.733	MWh/ton.CO_2	62,72
LT DAC	0.25/0.63	MWh/ton.CO_2	61,72
MeOH	0.17/0.44	MWh/ton.MeOH	62
H_2 for MeOH	0.2	ton/ton.MeOH	62
MeOH for CO_2 capture	0.685	ton/ton.CO_2	62
CO_2 emissions during MeOH utilization	1.37	ton/ton.MeOh	62

the respective equipment. Similarly, the fixed operating costs (FOCs) of each subsystem are calculated in Eqs. (30)–(32), respectively.

$$FOC_t^X = N^X \cdot PE_{MAX}^X \cdot C^{FOC.X} \tag{30}$$

$$FOC_t^{ELE} = N^{ELE} \cdot PE_{MAX}^{ELE} \cdot C^{FOC.ELE} \tag{31}$$

$$FOC_t^{BESS} = N^{BESS} \cdot PE_{MAX}^{BESS} \cdot C^{FOC.BESS} \tag{32}$$

Here, C^{FOC} represents the respective fixed cost of equipment, N with an equipment superscript represents the lifetime of the respective equipment, and PE_{MAX} with an equipment superscript represents the upper limit of electricity given to or provided by the respective equipment.

Case study and system description

Data gathering

The year 2020 was considered as the model basis with only four years of life span, considering the bitcoin algorithm's rewarding system, which halves the mining rewards every four years. If the analysis period exceeds this time span, uncertainty for difficulty level, total mining hash rate, and bitcoin prices would be significant. The solar irradiation, wind speed, and electricity price data for all US states were collected from multiple sources for comparison. Solar data was collected from the system advisor model (SAM) [40]. Wind speed data was collected from visual crossing [41]. The hourly average monthly electricity cost was collected from the US Energy Information Administration (EIA) and extended for yearly values, as shown in Figure S1 [42]. To calculate the annual CO_2 emission for the respective state, the resource mix percentage was collected from the US Environmental Protection Agency (EPA) [43]. Figure S2 illustrates the wind speed, capacity factor, and renewable/fossil mix percentage trends contributing to the cumulative grid power generation across various US states.

Bitcoin mining farm

A mining farm capacity of 360,000 TH/s was considered for this study. Bitmain Antiminer S19j Pro with a hashing power of 100 TH/s was considered as the mining equipment [44]. The mining revenue was determined as shown in Eq (33) below

$$\pi^{Bitcoin} = \frac{Price^{Bitcoin} \cdot R \cdot H \cdot t}{D \cdot 2^{32}} \tag{33}$$

where $\pi^{Bitcoin}$ is the revenue from bitcoin in USD, $Price^{Bitcoin}$ is the market price of bitcoin, R is the amount of bitcoin earned as a reward, i.e., 6.5 bitcoins, H is the hash rate, t is the mining time in seconds, and D is the network difficulty to mine. Bitcoin mining difficulty refers to how difficult it is to mine a block in a blockchain for bitcoins. A higher difficulty implies that it takes additional computing power to verify transactions. Therefore, in this study, using the average difficulty level for the year 2021 and the size of the mining facility, the yearly expected bitcoins were calculated [45]. The distribution of the mining difficulty for the year 2021 can be seen in Supplementary Figure S3. The profits from the total bitcoins mined in the year 2021 were then reported as a single value. The overall profits from bitcoin mining were then varied to find the BESP, i.e., the price at which net present value (NPV) becomes zero. Since the profit or the NPV based on the hourly bitcoin price would not be a useful measure, we reported the BESP of bitcoin in this study [46].

Each miner consumed about 3050 Watts. A linear correlation was assumed between the number of miners and their total power requirement. Apart from the mining power, the power values required for lighting and humidifiers (2% and 3% of the total mining power, respectively) were also considered in the calculations. For the mining farm, partial waste heat was assumed to be recovered [47], and HP were used to provide the cooling demands of the mining farm. We incorporated the energy recovery factor (ERF) in the analysis, which is the ratio of the energy reuse to the data center's total energy. Like the energy reuse effectiveness, the ERF refers to energy reuse calculated as the ratio of the energy used outside the control volume to the total energy used within the control volume. In this study, the amount of reusable heat recovered from the mining facility was assumed to be 0.22, based on a reference with a similar scale [48]. The waste heat recovered was subtracted from the total cooling demand and hence dealt with as the actual energy needed for the bitcoin mining facility operation. Based on the number of miners and their power consumption, the power required for cooling, and the miscellaneous power requirement (i.e., lighting and humidifiers), the total power demand for the mining facility was calculated. The power source for the mining farm included grid, solar, and wind power. Their respective share in the total power supplied to the mining farm was optimized to minimize the TAC and carbon emissions. While conducting economic analysis, the optimal number of resources utilized was used as a basis for TEA.

DAC system

This journal is © The Royal Society of Chemistry 20xx

Energy Environ. Sci. 2021, **00**, 1-3 | **7**
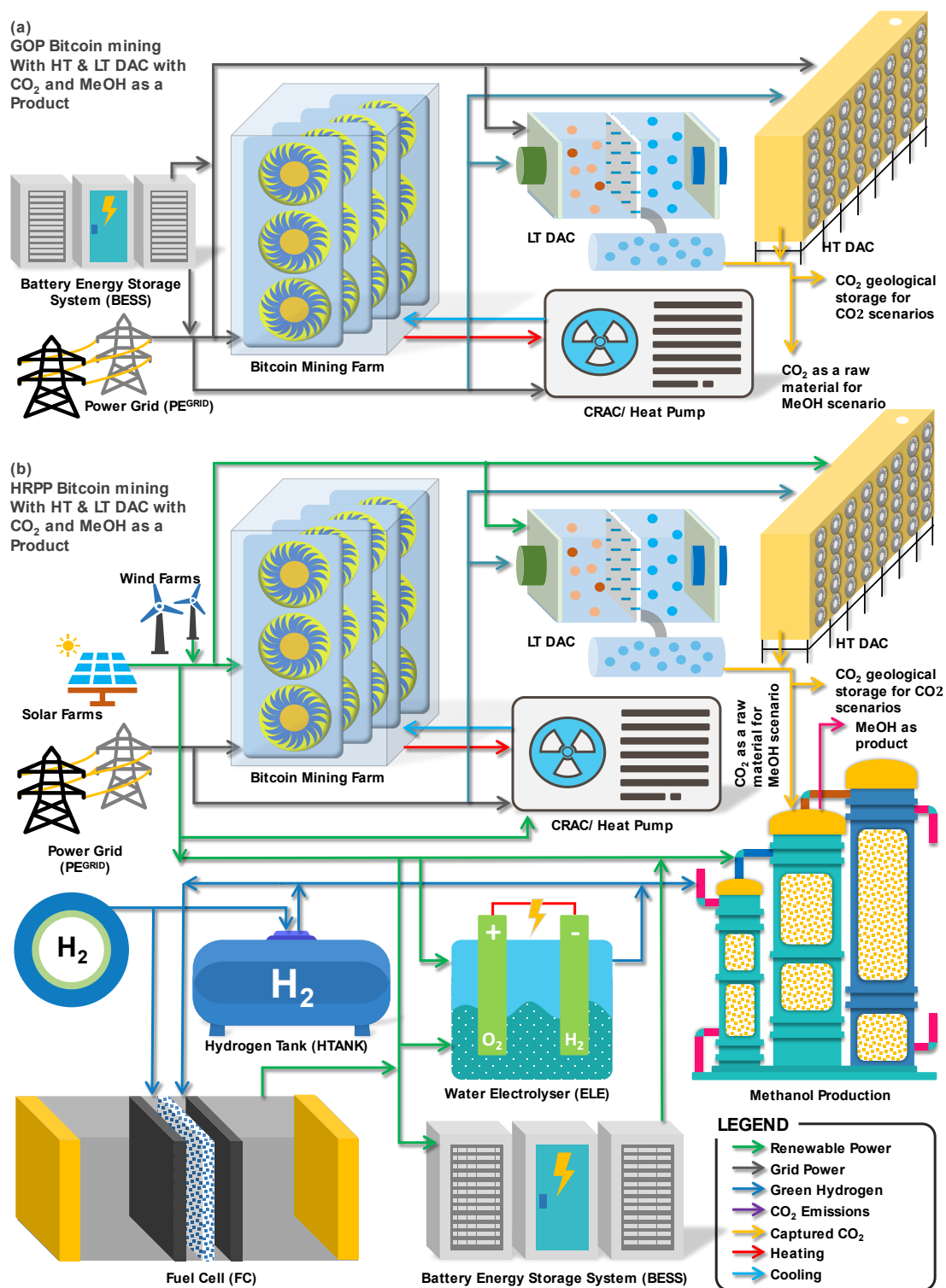
Figure 2. (a) GOP bitcoin mining with high-temperature (HT) and low-temperature (LT) direct air capture (DAC) with CO_2 capture and storage and MeOH as products, (b) HRPP mining with HT- and LT-DAC and CO_2 capture and storage and MeOH as products.

HT-DAC and LT-DAC systems were considered in the study. HT-DAC systems are mainly liquid-based systems consisting of two cycles, i.e., absorption and regeneration. As the name suggests, an HT-DAC system is a more energy-intensive process than an LT-DAC system. However, HT-DAC systems can handle large capacities of CO_2 capture [29]. Solid sorbents were used for LT-DAC systems to adsorb CO_2 on the sorbents and then desorbed when subjected to low temperature, depending upon the sorbent material. The parameters for the HT and DAC used in the study are shown in Table 1.

Methanol production

For the methanol production case scenario, it was considered that the methanol plants consume hydrogen generated from the electrolyzer and CO_2 captured from the DAC plant. For the renewable case scenarios, green hydrogen supply was considered to meet the methanol's hydrogen demand. Linear relations were considered to evaluate the thermal and electrical requirements and are mentioned in Table 1.

Other system components

Other components to meet the system's electrical, thermal, and cooling loads include ELEs, FCs, HPs, HTs, and BESS, as shown in Figure 2. For the GOP scenario, hydrogen was produced via electrolyzers, while hydrogen was assumed to originate from a biofuel plant for the HRPP scenario.

Economic assessment

Various economic assumptions were made during model development, as detailed below:

I. The system had a lifetime of 4 years.
II. No faults or delays were modeled; however, operation and maintenance costs were included.
III. Issues related to power dispatch were not considered in the analysis. Besides the cost of power inverters, converting direct current (D.C.) to alternating current (A.C.) was included in the equipment CAPEX [49–51].
IV. All equipment were assumed to be salvaged after the project life, except for mining equipment. The equipment's salvage values were calculated based on the remaining value of the equipment using the double-declining depreciation method [52–54]. The relations used for the calculation can be seen in Eqs. (34)–(38).
V. The interest rate considered in the study was 4.5%; however, to see the impact of relatively risky businesses, a higher interest rate of 20.0% was also subjected for analysis in the sensitivity analysis [55–57].
VI. An incentive of 85\$/ton of CO_2 captured and stored was considered in the analysis [58].
VII. The energy consumption of the bitcoin facility considered in the study was much lower than the total load for each state; hence, it was assumed that the additional bitcoin load would not affect the energy mix. Thus, only the average emission factor for fossil resources was chosen instead of the marginal emission factor.
VIII. For cases with CO_2 capture and storage, it was assumed that geological sites were within 100 km from the mining facility [59], and costs for CO_2 storage and transport were considered in the analysis [60].
IX. The purchase price of electricity for all US states was taken as hourly monthly average values and collected from EIA [42]. The power grid composition was taken as constant.
X. The sale of oxygen was not considered as the produced volume would saturate the market.

$$Depreciation\ per\ year = Book\ value \cdot Depreciation\ rate \tag{34}$$

$$Depreciation\ for\ the\ year = (Asset\ Cost - Salvage\ value) \cdot Factor \tag{35}$$

$$1^{st}\ year: Factor = \frac{NY^X}{1+2+3+\cdots NY^X} \tag{36}$$

$$2^{nd}\ year: Factor = \frac{NY^X - 1}{1+2+3+\cdots NY^X}\ uptill\ the\ last\ year \tag{37}$$

$$Last\ year: Factor = \frac{1}{1+2+3+\cdots NY^X} \tag{38}$$

Test system

In total, eight case studies were demonstrated, considering different types of power sources (GOP and HRPP), DAC technologies (HT and LT), CO_2 capture and storage, and the product type (MeOH). An overview of the scenario-wise schematic can be seen in Figure 2 with a detailed description as follows:

I. GOP mining for HT-DAC and CO_2 capture and storage
II. GOP mining with LT-DAC and CO_2 capture and storage
III. GOP mining with HT-DAC and MeOH as a product
IV. GOP mining with LT-DAC and MeOH as a product
V. HRPP mining with HT-DAC and CO_2 capture and storage
VI. HRPP mining with LT-DAC and CO_2 capture and storage
VII. HRPP mining with HT-DAC and MeOH as a product
VIII. HRPP mining with LT-DAC and MeOH as a product.

The details for economic parameters used in this study are detailed in Table S1.

Results and discussion

GOP mining with HT-DAC and CO_2 capture and storage

Calculations were performed to evaluate the annual costs of meeting the energy demands of the bitcoin mining farm. The
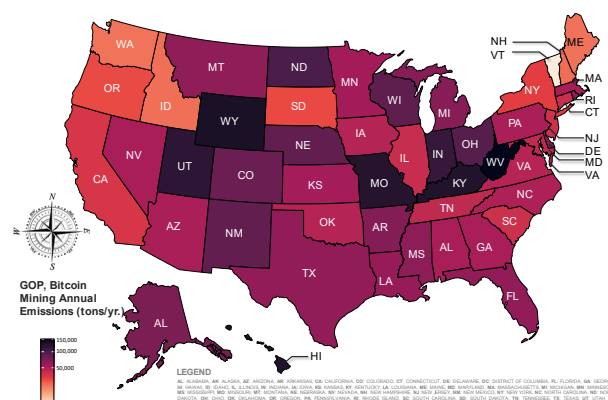
Figure 3. CO_2 emissions for the US states when powering the bitcoin mining farm using grid power.

power consumed by a bitcoin mining farm was constant for all states, considering a fixed mining farm capacity. The power consumed by the bitcoin mining farm accounted for a total of 16.98 MWh with 64.7% accounting for the mining farm, and the remaining 35.3% accounting for the cooling system and miscellaneous equipment (lighting and the humidifiers). To evaluate the electricity cost of powering the mining farm using the grid electricity, the annual electricity consumption was multiplied by the annual cost per kWh of power consumed. Figure S1 illustrates the average monthly electricity cost ($/yr.) for each respective state, whereas a yearly cost is mapped for per kWh of power consumption in Figure S4. The states with higher electricity prices cost more for bitcoin mining. Hawaii is the most expensive state in terms of electricity cost for grid-based mining, followed by Rhode Island and Alaska. In addition, the states with more renewable penetration in the grid tend to be among those with higher costs due to higher electricity prices. On the contrary, the states with more fossil fuel-based power penetration resulted in lower yearly electricity costs. Therefore, states like Oklahoma, Louisiana, and Montana had lower costs. Despite higher mining costs for states with higher renewable penetrations, these states had lower costs for CO_2 capture as the total emission for greener states had lesser emissions in comparison to states with more fossil fuel share and lower electricity prices. Figure 3 shows the amount of CO_2 emissions from each state when running on grid-based power. The states with higher renewable penetration in the grid, i.e., Vermont, with almost 99% of renewable power penetration was green due to a minute amount of emissions from fossil-based power, followed by South Dakota, Maine, Idaho, Washington and Oregon with renewable penetration percentages of 80.5%, 77.6%, 76.1%, 75.1%, and 67.5%, respectively, where the majority of the grid power was contributed by renewable sources. In Figure 3, the states with a darker red shade had the lower renewable resource mix in the grid and, as a result, the highest CO_2 emissions. The states with the highest emissions include West Virginia, Wyoming, Hawaii, Kentucky, Missouri, and Utah with almost 87.5% of the grid power contributed by fossil fuels.

Based on the yearly emissions from each state, the HT-DAC plant's energy and thermal requirements were calculated using

Figure 4. Break-even selling price of bitcoin (BESPBit) for HT-DAC with CO_2 capture and storage using GOP mining.

linear relations, and parametric values explained in Table 1. The HT-DAC plants consumed more power in comparison to the LT-DAC plants. The electrical and thermal power consumption for each state can be seen in Table S2. It can be observed that Vermont is 99% green and has almost no requirement for the HT-DAC plant as there is not enough emission throughout the year to capture. Similarly, Washington, Idaho, Maine, and New Hampshire had relatively lower power requirements in comparison to other states. For this scenario, all power supply came from the grid; thus, the cost incurred for the electricity consumption was the major contributor toward the OPEX besides the OPEX for DAC, HP, and CO_2 storage and transport. For the GOP scenario, as the total power came from a mix of renewable and non-renewable resources, the electricity consumed for the process contributes toward emissions despite capturing the emitted CO_2 using HT-DAC. Therefore, the net CO_2 emission was calculated for the states to evaluate whether they are still carbon-positive, carbon-negative, or carbon-neutral. Table S2 highlights the operational, economic, and resulting net CO_2 emissions results for all states for GOP with HT-DAC scenario. Lastly, the BESPBit was evaluated to determine which states would be profitable after including carbon initiatives in their investment plans while protecting both the environment and economy. Figure 4 illustrates the BESPBit values for all US states. None of the states was profitable even with the current bitcoin market value of 47,454.10 $ (Price on April 13, 2022, at 03:04 PM UTC). For the GOP scenario, it was seen that all the states were above the current market price of bitcoin, making all these states not profitable on today's date. Hawaii, Alaska, Rhode Island, Massachusetts, Wyoming, and West Virginia were the worst performing states with the current bitcoin market price. Furthermore, with additional emissions from the DAC plant, the overcall case scenario becomes carbon-positive with Vermont having the lowest CO_2 emissions among all states.

GOP mining with LT-DAC and CO_2 capture and storage

In comparison to HT-DAC, LT-DAC has 25.4% and 63.9% lesser electrical and thermal demand, respectively, giving it an economic advantage. However, an LT-DAC plant can process one-third of the capacity of an HT-DAC plant [29]. Table S3 summarizes the electrical and thermal demand for the LT-DAC plant along with the CAPEX and OPEX for respective states and net CO_2 emission per state. Results for LT-DAC are similar to HT-DAC besides the fact that due to a decrease in the electrical and thermal consumption, an overall 35.5% decrease and 8.1% increase were seen in the CAPEX and OPEX of the LT-DAC, respectively. From a CO_2 emissions perspective, like HT-DAC, LT-DAC was also carbon-positive, i.e., it emitted additional CO_2 while capturing. However, from an economic perspective, LT-DAC seems to be relatively safer based on the current bitcoin market price. Similar to HT-DAC, none of the states had the BESPBit less than the current market price of bitcoin. However, Idaho had a BESPBit of $53,533. While Tennessee, New York, Louisiana, Washington and Oklahoma had BESPBit less than Idaho, the lowest BESPBit was for Oklahoma i.e., $51,799. Overall, all states' BESPBit values were higher than the current market price. Figure S5 highlights the BESPBit for GOP LT-DAC
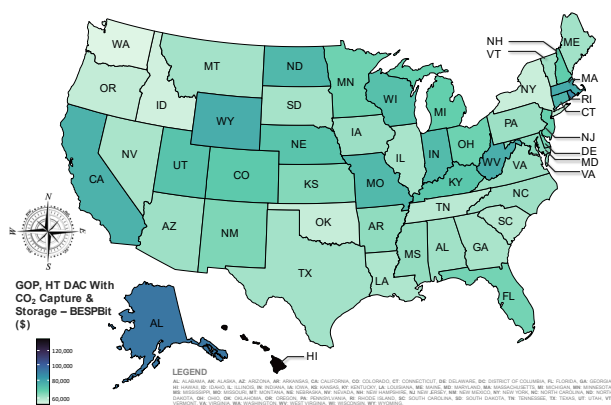
with CO_2 capture and storage scenario. Although the difference between the BESPBit of LT-DAC and that of HT-DAC is minor, a decrease in the minimum and the maximum values obtained for LT-DAC can be seen. For LT-DAC, Oklahoma had the lowest BESPBit, making Oklahoma the most favorable state for LT-DAC-based CO_2 capture and bitcoin mining.

GOP mining with HT-DAC and MeOH as a product

MeOH production requires hydrogen, which consumes around 48–54 kWh per kg of hydrogen [61]. Thus, besides DAC energy requirements, there is an additional power requirement by the hydrogen electrolyzer. For every ton of MeOH, about 0.2 tons of hydrogen is required. In the current scenario, we are looking to produce enough MeOH that can capture the amount of CO_2 that each state emits while mining bitcoins on the grid electricity. For each ton of CO_2 to be captured, 0.6849 tons of MeOH needs to be produced, and similarly, the hydrogen needed to produce equivalent MeOH comes from the water electrolyzer [62]. Overall, a significant contribution of electrical consumption comes from hydrogen production, which adds up to the total CAPEX and the OPEX. If we evaluate the electricity consumption, there are four major contributors, i.e., mining farm, DAC, MeOH, and hydrogen plant. Among these, hydrogen accounts for the highest share of 52.2%, followed by the mining farm with a total share of 32.09%, and the remaining accounts for the DAC and the MeOH plant. However, grid-powered facilities still give a tentative advantage over power-intensive facilities in locations where electricity is cheaper. States with an immense renewable penetration end up with lesser emissions and hence lesser investments for carbon capture. States with more renewable and relatively lower electricity prices emerge as potential options for mining farms with carbon capture initiatives. Overall, none of the states in the case of HT-DAC with MeOH as a product resulted in the BESPBit being lower than the current market price of bitcoin. Hawaii was the worst state for the current scenario with the BESPBit of $369,358, followed by Alaska, West Virginia, Rhode Island, Wyoming, Missouri, Indiana, North Dakota, Utah, and Kentucky. Figure S6 the state-wise distribution of the BESPBit for HT-DAC with MeOH as a product. It can be seen that the darker the state color, the higher the BESPBit. In addition, the minimum BESPBit for this scenario increased by 169.2% and 259.5% for the HT- and LT-DAC with CO_2 capture and storage, respectively. The state of Vermont was the one with the lowest BESPBit but was still not profitable enough being higher than the current market price of bitcoin, followed by Washington, Idaho, Oregon, New York, and Maine. Besides the economics, it must be noted that all states emitted more than they captured for the MeOH case. The detailed list can be seen in Table S4. Washington, Maine, Idaho, New Hampshire, and Oregon were among the states with the lowest emissions after Vermont.

GOP mining with LT-DAC and MeOH as a product

Similar to LT-DAC with CO_2 capture and storage, LT-DAC with MeOH as a product also had a similar trend when compared with their respective HT-DAC scenarios. As explained in the previous sections, HT-DAC cases are electrically and thermally
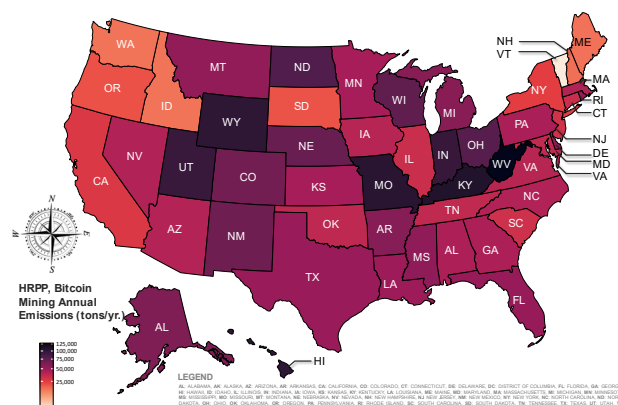
Figure 5. CO_2 emissions for the US states when powering bitcoin mining farm using HRPP energy.

intensive processes, whereas LT-DAC has lower electrical and thermal power consumers. For LT-DAC with MeOH, the number of states with the BESPBit higher than the current bitcoin market price remained the same. Hawaii was again the worst state for the current scenario followed by Alaska, Rhode Island, West Virginia, Wyoming, Missouri, Indiana, North Dakota and Utah. 0.7% and 9.0% drops in the minimum and maximum values of BESPBit for LT-DAC with MeOH were seen compared to the HT-DAC with MeOH case. The state-wise distribution of the BESPBit can be seen in Figure S7 with a detailed description of the energy consumption, CAPEX and OPEX, and the net carbon capture in Table S5. The number of states with a net positive carbon capture was similar to the HT-DAC with MeOH case. The list includes Idaho, Maine, New Hampshire, South Dakota, Vermont, and Washington with net positive CO_2 capture.

HRPP mining with HT-DAC and CO_2 capture and storage

Unlike GOP cases described in the previous sections, for the HRPP case, an optimization problem was formulated to evaluate the optimal number of solar panels, wind turbines and the grid share to meet the energy demands of the bitcoin mining farm. A combination of grid and renewable case scenarios was considered as realistically as possible, keeping in
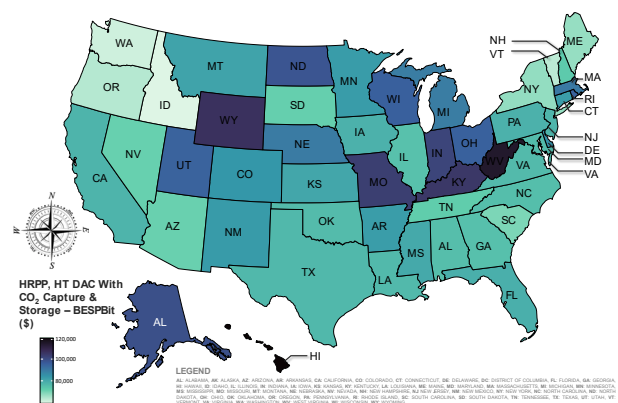
Figure 6. Break-even selling price of bitcoin (BESPBit) for HT-DAC with CO_2 capture and storage with the HRPP scenario.

This journal is © The Royal Society of Chemistry 20xx

Energy Environ. Sci. 2021, **00**, 1-3 | **11**
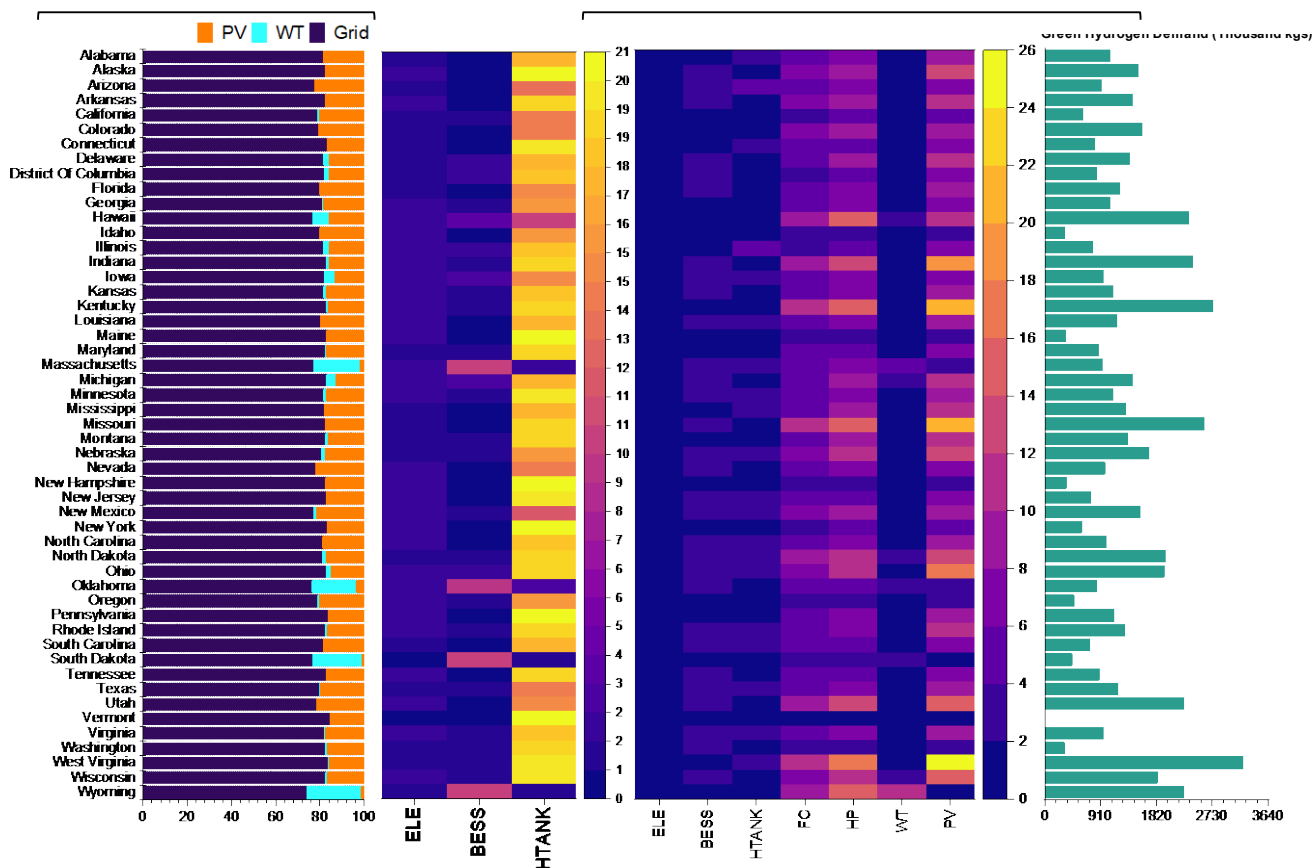
Figure 7. US state-wise PV, WT, grid resource mix, the optimal numbers of BESS, WTs, and PVs required to power bitcoin mining farm, and the optimal numbers of ELE, BESS, HTANKs, FCs, HPs, WTs, PVs, and hydrogen required to power the HT-DAC plant for the HRPP scenario with CO_2 capture and storage. The BESS, PV, ELE, FC, and HP have a 1.0 MW rating, whereas the WT and HT have 1.6 MW and 10 kg ratings.

mind huge investments needed to meet the high energy demand of the mining farms. The power consumed by a bitcoin mining farm was constant for all states, considering a fixed-capacity mining farm for all states. The power consumed by the bitcoin mining farm accounted for a total of 16.98 MWh, with 64.7% accounting just for the mining farm and the remaining 35.3% accounting for the cooling system and miscellaneous (lighting and the humidifiers). An optimization program was run to evaluate the share from solar panels, wind turbines, and the grid to meet the energy demand of the mining farm. Figure S2 shows the grid resource mix distribution. Some states had their majority grid power coming from renewables, whereas others had the most share coming from non-renewable resources. The amount of CO_2 emissions was evaluated for each state using the data for grid resources for each respective state. States such as Vermont, which has 99% renewable power mix, would require a minimum contribution for carbon capture or no need for it to be highly renewable. Similarly, states like Delaware may need a considerable investment as all power is mainly supplied from the non-renewables, resulting in more efforts needed for carbon capture, making these states less favorable for investments in bitcoin mining. However, the type of fossil fuel source that contributes to the grid makes a huge impact. Delaware has the highest fossil mix i.e., 97.5% non-renewables, however, the major contributor to Delaware's fossil mix is

natural gas, which has relatively lesser emissions as compared to coal. Therefore states like West Virginia, Wyoming, Missouri, Kentucky and Utah with a higher coal contribution in the fossil mix account for the highest emissions and as a result are among the states with the highest BESPBit. Apart from the renewable and non-renewable debate, interesting results for the HRPP scenarios were observed. The grid electricity cost and solar and wind resources in a particular location play a vital role for each state. These numbers further derive the best and worst state-wise scenarios for profitable and sustainable mining. A summary of the optimal values obtained to power the mining farm using a grid mix, and renewable power is shown in Figure 7. States with good solar capacity and wind speed tend to have lesser PV panels and WTs respectively.

In comparison, states with good wind speed had more WTs rather than PV panels. Besides this, states with relatively higher electricity costs also tend to employ BESS for energy storage. States with good potential for neither PV nor WT tend to go with the one with lower investment costs or rely on the grid resources alone. Notably, the carbon tax was also included in the objective function along with the cost for the investments in renewable energy and grid resources. Thus, all the states preferred to use grid resources along with some states choosing between PVs, BESS and WTs. So, even if states with a high renewable share in the grid opt for the grid electricity as an

12 | *Energy Environ. Sci.* 2021, **00**, 1-3

This journal is © The Royal Society of Chemistry 20xx
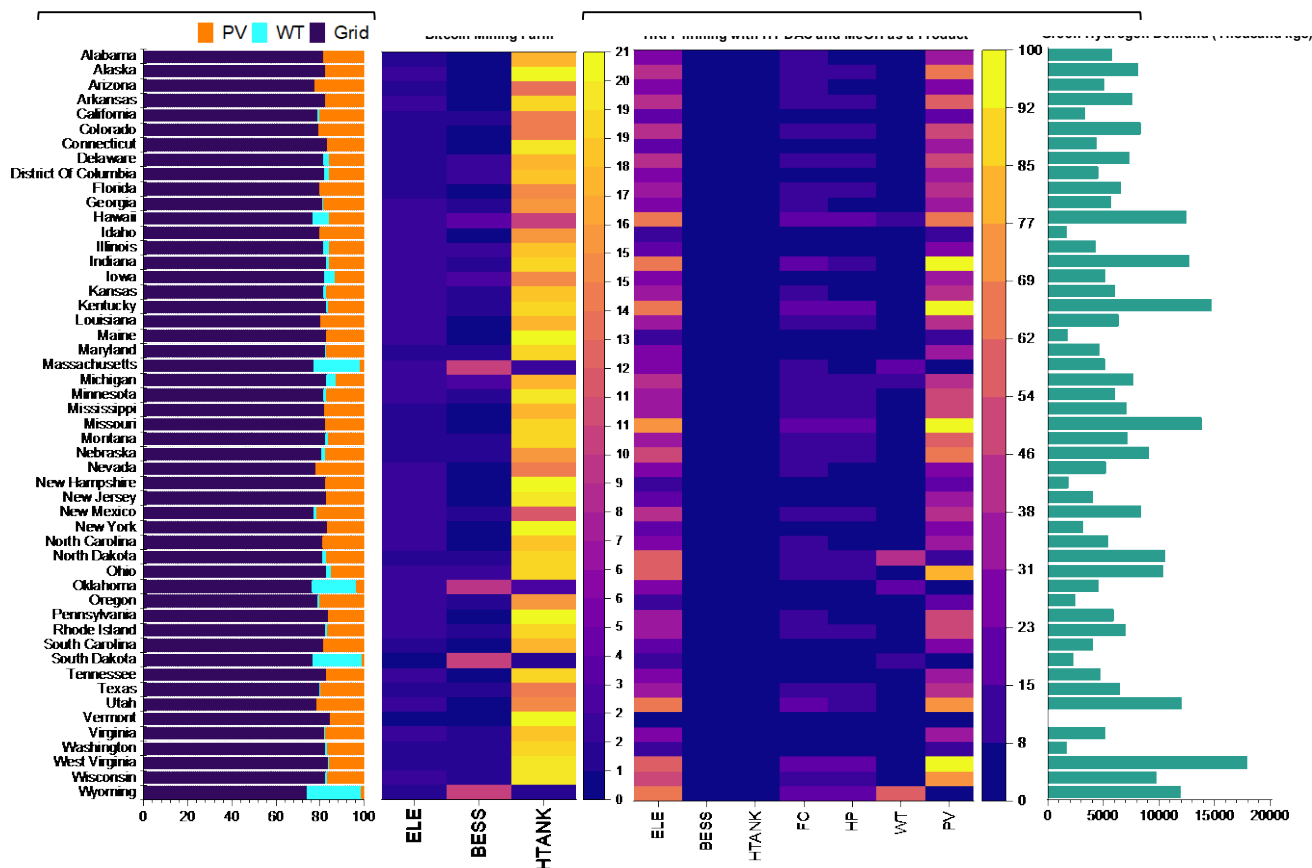
Figure 8. US state-wise PV, WT, and grid resource mix, the optimal numbers of BESS, WTs, and PVs required to power the bitcoin mining farm, and the optimal numbers of ELE, BESS, HTANKs, FCs, HPs, WTs, PVs, and hydrogen required to power the HT-DAC plant for the HRPP case with MeOH as a product. The BESS, PVs, ELE, FCs, and HPs all have a 1.0 MW rating, whereas the WTs and HTANKs have a 1.5 MW and 10 kg rating.

optimal choice, they pay a lower carbon tax than what they would have invested in the renewables.

As of now, there is a reduction in the share of electricity coming from the grid, which results in the reduction of CO_2 emissions. So, the emissions from the use of the grid electricity were recalculated; consequently, the equivalent amount of power required to meet the HT-DAC plant electrical and thermal power was recalculated. The model was optimized using the updated values and the objective function, as shown in Eq. (2), but this time with a complete renewable scenario. The FCs, ELE, BESS, and HTANKs were considered as power, hydrogen, and energy storage options for a complete renewable optimization scenario. It was assumed that the green hydrogen is supplied from a renewable hydrogen plant to meet the FC's hydrogen demand and an electrolyzer for on-site hydrogen production. Results from the optimization of electrical and thermal demands in the HT-DAC case can be seen in Figure 7. West Virginia, Kentucky, Rhode Island, Delaware, Indiana, Missouri, Louisiana, Mississippi, and Ohio were among the ones with a relatively higher hydrogen consumption owing to their higher emissions as non-renewables mainly constitute their grid electricity. With no grid power supply and an effort to be renewable, huge investments and additional resources are required to contain surplus energy as a backup. Using the optimal numbers of equipment needed to make HT-DAC

completely renewable, economic results were generated while taking into account the CAPEX, fixed and variable operating and maintenance costs for each piece of equipment, and cost for the renewable hydrogen used to generate power via FCs. A detailed overview of emissions from each state, CAPEX and OPEX, and net carbon capture after going renewable can be seen in Table S6. The emissions have already been reduced when using renewables and the grid mix. For states like Vermont, a total of 162.73 tons/yr was observed, indicating that even without a CO_2 capture facility, Vermont will still be a favorable choice for bitcoin mining. A visual distribution for CO_2 emissions from HRPP mining can be seen in Figure 5.

Furthermore, the net CO_2 emission was the same as the one emitted from the bitcoin mining farm as the HT-DAC scenario was entirely powered via renewables. States with lesser than 14,000 tons/yr of CO_2 emissions besides Vermont include Washington, Idaho, Maine, New Hampshire, and South Dakota. The BESPBit for the HRPP cases for HT-DAC with CO_2 capture and storage can be seen in Figure 6. It can be observed that moving from the GOP scenarios with HT and LT-DAC with CO_2 capture and storage and MeOH as a product to HRPP scenarios, respectively. The color intensity increases and gets darker due to the shift of the BESPBit from a much lower level of $51,799 to a new minimum of $61,798 for the HRPP case, an increase of 19.3%. Hawaii is the state with the highest BESPBit, followed by

This journal is © The Royal Society of Chemistry 20xx

Energy Environ. Sci. 2021, **00**, 1-3 | **13**
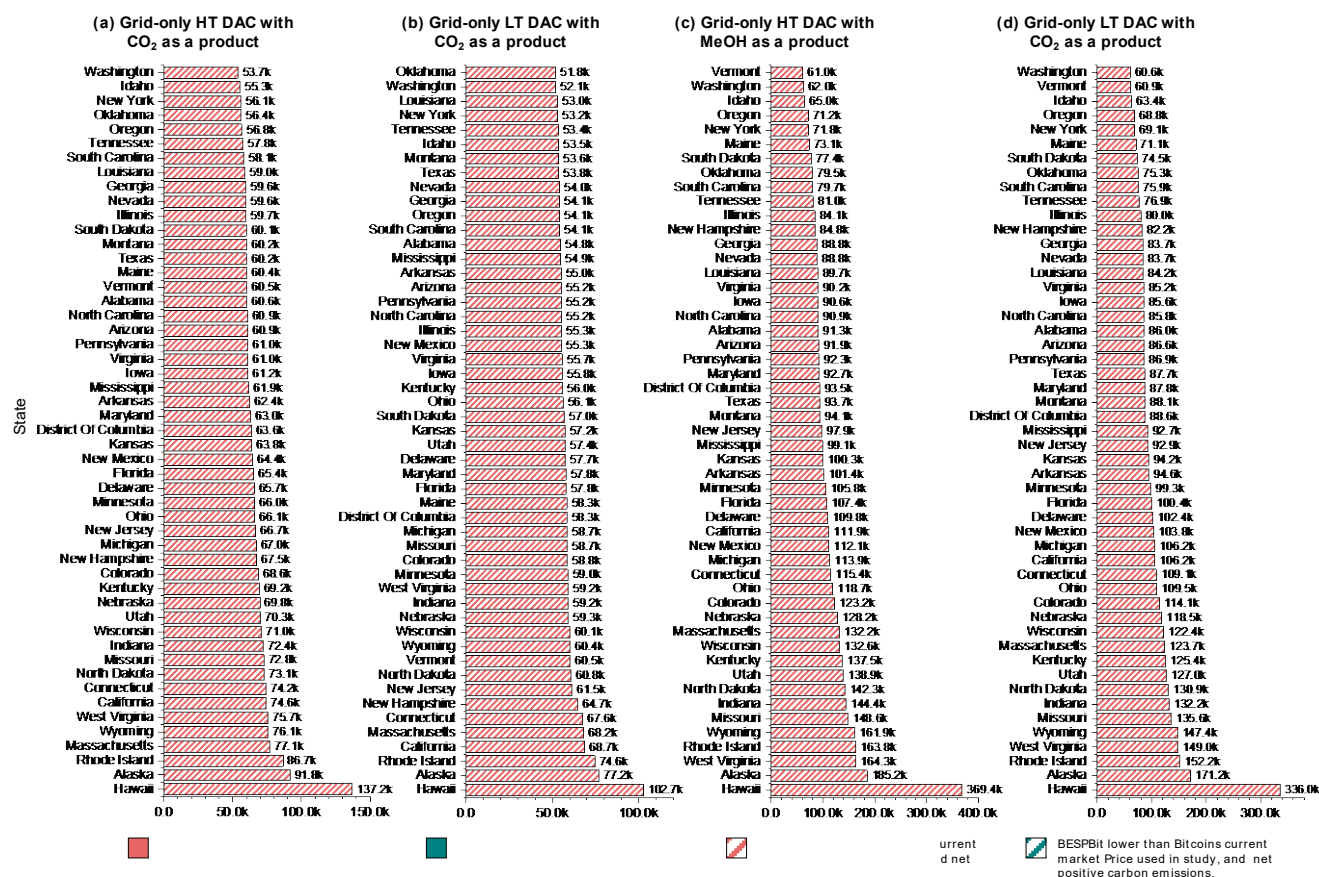
Figure 9. Best and worst states from BESPBit and carbon emissions perspective for the GOP case.

West Virginia and Wyoming. The states with the lowest BESPBit but still not profitable happened to be Idaho, Washington, Vermont, Oregon, and Maine, followed by other states, as shown in Figure 6. Besides the fact that all states were carbon-neutral, none of the states' BESPBit were below the current market price of bitcoin. Like HT-DAC, only LT-DAC HRPP scenarios were carbon-neutral as there were no additional emissions from CO_2 capturing and storage. However, MeOH utilization resulted in additional emissions and is therefore not considered as carbon neutral.

HRPP mining with LT-DAC and CO_2 capture and storage

Similar to HT-DAC and CO_2 capture and storage, the steps for evaluating the optimal numbers of PVs, WTs, BESS, and the grid electricity share for powering the bitcoin mining farm, and the optimal numbers of PVs, WTs, ELE, FCs, HTANKs, BESS, and HPs for the HRPP scenario were similar. For LT-DAC, similar to the previous cases, LT had lower electrical and thermal consumption in comparison to HT-DAC. Therefore, the number of resources required to meet the electrical and thermal demand was also reduced. But the optimal value for the PV, WT, and BESS resources was similar, as described in Figure 7, as the mining farms' consumption remains the same. The distribution of optimal values obtained from the optimization model for powering LT-DAC can be seen in Figure S8. Vermont is the only state with no requirement for PVs and WTs. The total electrical and thermal demand was met using green hydrogen, FCs, and

HPs. All the states were carbon-neutral. A detailed overview of the emissions from each state, CAPEX and OPEX, and the net carbon capture after going renewable can be seen in Table S7. The resource distribution for LT-DAC changed completely compared to HT-DAC, considering lower electrical and thermal demand. Overall, the number of units for each decreased or increased based on overall optimization decisions. HRPP LT-DAC with CO_2 capture and storage also had none of the states below the current market price of bitcoin and can be seen in Figure S9. The states become darker as we shift from the grid to renewable scenarios. The overall BESPBit minimum prices for the HRPP LT-DAC scenario among all the states reduced from $61,789 to $58,613, i.e., a 5.2% decrease from the HT-DAC with an HRPP scenario.

HRPP mining with HT-DAC and MeOH as a product

The electrical and thermal demand was further raised for the grid and renewable-powered mining with HT-DAC and MeOH as a product. Although hydrogen was assumed to be coming from the grid, there was still an option to generate on-site hydrogen. On-site hydrogen generation would have cost quite more, considering the cost of the renewable infrastructure needed and electrolyzers with a higher capacity. In contrast, buying hydrogen from the market would be a much more reasonable option to opt for. Although more investment was needed to produce MeOH, the value of the product was higher as compared to the carbon capture and storage incentive.
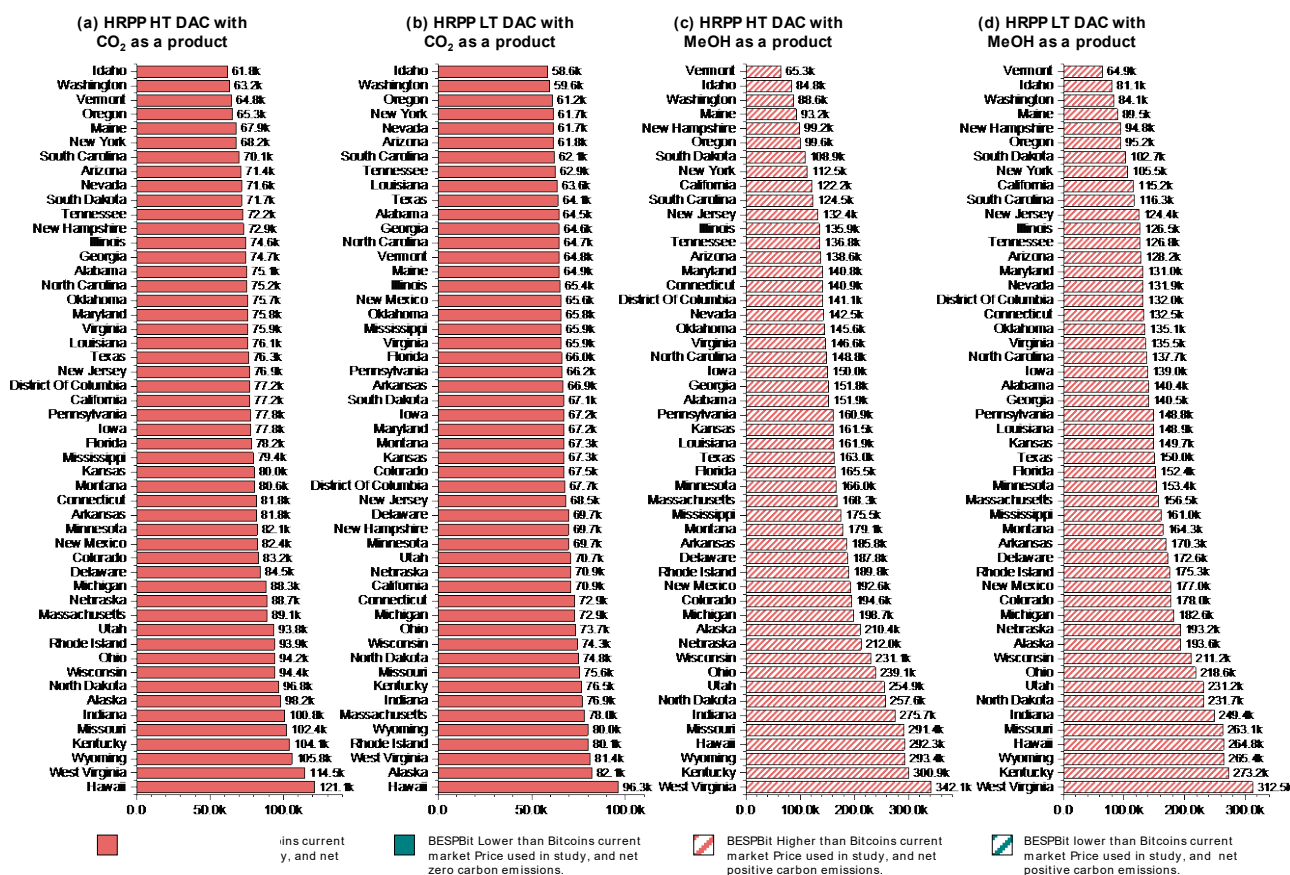
Figure 10. Best and worst states from the BESPBit perspective for the HRPP case.

However, the question was whether MeOH production at such capacities can generate profit or not, considering the market price of bitcoin and MeOH. As the bitcoin price largely fluctuates, it would be a risky investment as a slight increase or decrease in the bitcoin market price can make huge differences in investment return. The optimal values for the PV, WT, and BESS resources are described in Figure 8. Figure 8 also highlights the resource distribution to meet the electrical and thermal demand of the mining farm. N^{FC} was seen to be the most frequently used equipment as the FC was the alternate power source besides the PV and WT. In case when the PV and WT or either of their power is not available, FC can support the electrical demand. States like Kentucky, Missouri, West Virginia, Indiana, Ohio, Wisconsin, and Utah were the ones with the highest N^{PV}. West Virginia, Kentucky, Missouri, Hawaii, Indiana, and Wyoming had the highest hydrogen consumption with a detailed list shown in Figure 8. If we want to evaluate the increase in the CAPEX with GOP HT-DAC and MeOH as a product, taking the state of Alabama as an example, a 66.4% increase was observed. It clearly states that HRPP bitcoin mining with MeOH as a product will not be an economic investment considering higher CAPEX and lower production; only an equivalent amount of MeOH was produced to accommodate the emitted CO_2 during mining. However, owing to higher CAPEX and OPEX, as shown in Table S8, none of the states managed to be on the economic side. Figure S10 shows the BESPBit for the HT-DAC plant with MeOH as a product.

HRPP mining with LT-DAC and MeOH as a product

Although MeOH has an additional power requirement, which means additional cost for the infrastructure, with LT-DAC, these requirements are cut short but with an added disadvantage of handling one-third of the capacity that an HT-DAC can oversee. Overall, the costs for LT-DAC with MeOH as a product with grid and renewable case scenarios are reduced, but not to the extent that additional states also appear profitable. Apart from the mining farms' requirements for the PV, WT, BESS, and HP, requirements to power the LT-DAC plant were slightly lesser than those for the HT-DAC MeOH plant. The details can be seen in Figure S11. A few states relied totally on the PV or WT with additional power demand supplied via the FC using green hydrogen from the market. Like HT-DAC, LT-DAC also had similar states with the highest N^{PV}, N^{WT}, and N^{FC} units. A detailed description of the CAPEX and OPEX and the net CO_2 emissions can be seen in Table S9. All states were carbon-positive, and none of the states were below the current bitcoin market price considered in the study owing to the high investments needed for the renewable case scenario. Figure S11 shows a distribution of the BESPBit for the LT-DAC plant with MeOH as a product with a HRPP scenario. It must be noted that there was not much difference in the lowest BESPBit value, but for the maximum value, a decrease of 8.63 % was observed for the BESPBit in the current scenario.

Comparative analysis

The previous sections describe in detail the optimal equipment configurations, CAPEX and OPEX, and how each state performs when it comes to economics and the environment, i.e., CO_2 net emissions. Here, an overall comparison is drawn for the best- and worst-performing states scenario-wise and how often a particular state appears as a favorable option for a prospective investment. Figure 9 and Figure 10 show the best and worst states from the BESPBit perspective for GOP and HRPP scenarios, respectively. It was observed that the state of Washington, Idaho, New York, and Oklahoma were the only ones that appeared with the BESPBit lower than $57,000 for the GOP scenario with HT-DAC and CO_2 capture and storage. Whereas for the GOP LT-DAC with CO_2 capture and storage only twenty-five states were below the $ 57,000, however still higher than the current bitcoin market price. These states included Oklahoma, Washington, Louisiana, New York, Tennessee, Idaho, Texas, and Nevada, followed by others, as shown in Figure 9. All the remaining case scenarios turned out to be not economical and, in some cases, even not environmentally friendly. It was evident that only the GOP scenarios with CO_2 capture and storage were relatively economical. For HRPP scenarios with CO_2 capture and storage, despite being environmentally friendly, all the states had higher BESPBit with the lowest BESPBit for Idaho i.e., $58,613. This reflects that bitcoin mining may become economically viable with a renewable power source in the future with the decrease in technology costs, but not at the current time owing to significant investments needed for renewable infrastructure. Also, considering the high fluctuations in the bitcoins price, there is a considerable risk associated too. However, new miners moving to US states may go with the GOP scenarios but whether or not they are willing to invest in carbon capture to mitigate the emissions is a question. Policymakers can develop policies that require capturing carbon with suitable incentives in place to encourage carbon capture along with GOP bitcoin mining or paying a carbon tax if miners use grid electricity, or incentivize the miners to use renewable electricity to help cover the costs and encourage green bitcoin mining. Sensitivity analysis further discusses the role of changing technology costs on the BESPBit for various cases.

Sensitivity analysis

The price of bitcoin changes merely with a single tweet from well-known influencers and public icons (e.g. by Elon Musk, when he mentioned he talked to "North American Bitcoin miners" [63]). Therefore, the bitcoin price is subjected to multiple uncertainties[64–66], making the bitcoin price prediction model unrealistic. Besides, the size of the bitcoin mining farm is fixed, meaning that dynamic pricing data would not be helpful as there are no decisions to be made on the size of the bitcoin mining farm facility. The constraints on the bitcoin pricing model would have been helpful if decisions were made on the size of the mining facility. Therefore, in this study, the bitcoin mining difficulty was used as a parameter to evaluate the variation in the BESP of bitcoin. Based on the bitcoin mining

difficulty distribution for the year 2021, as shown in Supplementary Figure S3, 25%–75% of the data lies within the range of 18.9 tera hash (TH) to 22.3 TH. Based on this distribution, we chose the sensitivity range for mining difficulties to evaluate the possible number of bitcoins mined each year based on the mining equipment hash rate and the mining difficulty [45]. Using the bitcoin mining difficulty rate, the value for the bitcoin mined was evaluated and used to calculate the BESP of bitcoins for each scenario. As the number of bitcoins did not influence the sizing parameters for DAC and MeOH, the overall percentage difference in the BESP was similar for all states and the respective case scenarios from their base values reported in the results. With the minimum mining difficulty of 14.3 TH taken as a reference from the above plot, a decrease of 15.9% was observed in the BESP for all states and the respective case scenarios, i.e., GOP and HRPP scenarios. With the maximum mining difficulty of 22.3 TH, the BESP increased by 47.14% for all states from the base value reported for the GOP and HRP scenarios. The states with a higher BESP had higher variations compared to those with lower BESP.

To see the impact of the interest rate on the BESP, the interest rate was evaluated at a minimum value of 4.0% and a maximum value of 20.0%. With an increase in the interest rate up to 20.0%, an increase in the BESP of bitcoins was observed from a minimum value of 4.0% up to a maximum of 30.0%, whereas, with a decrease in the interest rate, the BESP of bitcoins only changed by less than 1.0%. Hawaii followed by Rhode Island had the minimum change in BESP from their base values, as reported in the results section, at an interest rate of 20.0% as their BESP values were among the highest for all scenarios (i.e., GOP and HRPP)[56,67]. The results of the sensitivity analysis for the interest rate can be seen in Supplementary Figures S13 and S14. To further understand the impact of technology cost and efficiencies, the parameters were subjected to variations to evaluate the minimum and maximum variations in the BESP of bitcoins. The subjected parameter's sensitivities are provided in Supplementary Table S10. Among all parameters, the interest rate followed by the CAPEX of equipment, bitcoin CAPEX, DAC CAPEX, and DAC electrical and thermal requirements had a significant impact. The results of the sensitivity analysis can be seen in Figures S15–S22. The states with higher costs showed higher changes in their BESPBit based on the variations of the sensitivity parameters. These states include West Virginia, Wyoming, Wisconsin, Alaska, and Alabama, followed by other states.

Discussion

The potential future directions as well as the limitations of the study are discussed to further study this area and come up with more economical and environmentally friendly solutions to make bitcoin mining green and sustainable. Although PoW offers a more secure public network, it comes with excess energy consumption. In contrast, PoS requires less energy, making it impossible to identify the validators. Unlike in PoW, where miners are traceable due to high energy use, authorities can locate and shut down the mining facilities[10,11]. The study

PAPER

focused on evaluating and capturing the costs incurred by bitcoin mining for each state based on the GOP and HRPP scenarios. However, residual emissions exist for all processes, except for HRPP HT- and LT-DAC with CO_2 capture and storage. The residual emissions for GOP with CO_2 capture and storage and MeOH account for the emissions as a result of DAC via grid resources and MeOH utilization, respectively, whereas for the HRPP MeOH scenario, the emissions originate from the DAC process as well as MeOH utilization. However, these emissions were not considered in this study and hence need to be addressed in a future work. Besides energy-intensive processes, bitcoin mining generates 34.05 kt of electronic waste [68]. The amount of generated waste is comparable to the I.T. equipment waste of the Netherlands. Therefore, we will focus on the carbon neutrality and life cycle assessment of the bitcoin mining process in the future.

As the dynamic nature of renewable energy is well-known, sudden fluctuations likely disrupt the system. As a result of the high penetration of renewable energy in power grids, frequency stability and power quality issues occur. Besides, the power consumption of mining equipment as a type of load with certain fluctuations will also fuel the problem of power grids while adopting this scheme on a large scale. Even though power inverters are part of the CAPEX of solar equipment, they do not perform effectively. A harmonic filter can be used to manage the deviating frequency and voltage issues. In this study, power quality issues were not addressed, which is one of the study's limitations[50]. For this reason, it may be considered as a future research direction. In terms of power sources other than WT and PV, a hydrogen-powered bitcoin mining facility may be further investigated. Hydrogen can be produced from renewable sources at a price range of 9.0 to 11.0 \$/kg [69–71]. However, additional transportation and storage costs make the overall costs more expensive. Hydrogen-powered scenarios can present a favorable pathway with reductions in technology costs for the production, storage, and transportation of hydrogen. Despite higher technology costs, policymakers can introduce suitable incentives for green mining instead of putting restrictions on bitcoin mining.

Conclusions

It is quite concerning how bitcoin mining impacts the environment and energy supply. The boom in the bitcoin price has recently attracted remarkable attention while also causing the electricity demand and carbon emissions to increase. In search of cheaper electricity and more freedom in mining, miners are being moved to the US. However, concerns remain regarding economic and environmental integrity. Therefore, the study provides a comprehensive analysis of the technology of and investments in bitcoin in US states. This study examines bitcoin's economic and environmental standing across US states which may be considered mining sites due to their relatively cheap and green electricity. Initiatives like carbon capture and renewable-powered mining farms can provide a step toward sustainable mining. In addition, the study discusses potential profit margins for each state under a variety of scenarios by

comparing the BESPBit to the current bitcoin market price. The findings suggest that states with a high share of renewable energy in the grid and lower electricity prices could offer a solution. Carbon capture in these states is a relatively low-cost investment for investors, making it a more reliable investment for the environment. Washington was the most profitable state, followed by Vermont and New York. The states of Vermont, Maine, Washington, Idaho, and New Hampshire emitted less CO_2. Hawaii, Rhode Island, Alaska, Connecticut, West Virginia, and Kentucky were the worst states from an economic standpoint. In all scenarios, Delaware, West Virginia, Rhode Island, and Kentucky produced the highest amounts of CO_2 emissions.

The findings of the study will provide a holistic overview for policymakers to strategize for investor support as well as save the environment. Incentives for carbon capture and ecofriendly mining will benefit everyone if both policymakers and investors take appropriate actions. In addition, this work realistically estimates the economic and environmental benefits of carbon capture and renewable initiatives for realizing sustainable bitcoin mining only (i.e., PoW based crypto currencies).

Nomenclature

	Indices and acronyms
$ASIC$	Application-specific integrated circuits
$BESPBit$	Break-even selling price of bitcoin
$BESS$	Battery energy storage system
$CAISO$	California independent system operator
CCU	Carbon capture and utilization
CO_2	Carbon dioxide
CRF	Capital recovery factor
DAC	Direct air capture
DEG	BESS Degradation
ELE	Electrolyzer
EPA	Environmental protection agency
EIA	Energy information administration
GOP	Grid-only Powered
FC	Fuel cell
$GRID$	Grid
HP	Heat pump
$HRPP$	High renewable penetration powered
$HTANK$	Hydrogen storage tank
$HT\ DAC$	High Temperature Direct Air Capture
$LT\ DAC$	Low Temperature Direct Air Capture
IR	Inflation rate
M	Charging
$MeOH$	Methanol
$MILP$	Mixed-integer linear problem
P	Discharging
PoW	Proof of Work
PV	Photovoltaic solar panel
REN	Renewable
S	Steam
SAM	System advisor model
t	Index of time $t = 1,2,…,T$

This journal is © The Royal Society of Chemistry 20xx

Energy Environ. Sci. 2021, **00**, 1-3 | **17**

TAC	Total annual cost
TH	Terahash
w	Water
WT	Wind turbine
Parameters	
$C^{FOC.X}$	Fixed operating cost of $X = PV, WT, CCHP, FC, HTANK, HP$
C^{DEG}	Cost of BESS degradation ($/MWh)
C^{X}	Cost of $X = PV, WT, CCHP, FC, HTANK, HP$
C_H^{REN}	Cost of green hydrogen
COP^{HP}	Coefficient of performance of HP
$f_O . \pi_O$	Price of raw material ($/kg-H$_2$), $O = N_2, KOH, S, w$
H_{MAX}^{REN}	Maximum penetration for green hydrogen (kg)
H_{MIN}^{REN}	Minimum penetration for green hydrogen (kg)
LHV_H	Lower heating value of hydrogen
NY	Number of years
NY^{X}	Equipment life of $X = PV, WT, CCHP, FC, HTANK, HP$
OMC^{X}	O&M of $X = PV, WT, CCHP, FC, HTANK, HP$
$P_{e,t}$	Electrical and thermal power demand (MWh) at any given time t
PE_{MAX}^{ELE}	Upper limit of power for ELE
PE_{MIN}^{ELE}	Lower limit of power for ELE
PE_r^{WT}	Wind turbine rated capacity (MW)
PG_{MAX}^{GRID}	Minimum penetration from natural gas grid
PG_{MIN}^{GRID}	Maximum penetration from natural gas grid
r_t^s	Solar irradiance (W/m^2) at time t
RC^{X}	Replacement cost of $X = PV, WT, CCHP, FC, HTANK, HP$
S^{PV}	Solar panel surface area (m^2)
SOC_{MAX}^{BESS}	SOC upper limit for capacity in BESS
SOC_{MIN}^{BESS}	SOC lower limit for capacity in BESS
SOH_{MAX}^{HTANK}	SOH upper limit for hydrogen storage capacity in HTANK
SOH_{MIN}^{HTANK}	SOH lower limit for hydrogen storage capacity in HTANK
$v_r, v_t^s, v_{cout}, v_{cin}$	Rated speed, wind speed, cut-out speed, cut in speed (m/s)
$\eta^{C.M}$	Discharging efficiency for $C = BESS, HTANK$
$\eta^{C.P}$	Charging efficiency for $C = BESS, HTANK$
η^{ELE}	Efficiency of ELE
η^{FC}	Efficiency of FC
η^{PV}	Efficiency of PV
Variables	
ANC^{X}	Annualized cost of $X = PV, WT, CCHP, FC, HTANK, HP$
$C_t^{DEG.BESS}$	BESS degradation cost at any given time t
FOC^{X}	Fixed operational cost of $X = PV, WT, CCHP, FC, HTANK, HP$
$H_t^{HTANK.M}$	Hydrogen discharging to HTANK at any given time t
$H_t^{HTANK.P}$	Hydrogen charging to HTANK at any given time t
H_t^{ELE}	Hydrogen from ELE at any given time t
H_t^{FC}	Hydrogen to FC at any given time t

H_t^{LOAD}	Hydrogen load at facility at any given time t
H_t^{REN}	Renewable hydrogen imports at any given time t
N^{X}	Number of equipment $X = PV, WT, CCHP, FC, HTANK, HP$
$O\&M_t^{X}$	Variable O&M cost of $X = PV, WT, CCHP, FC, HTANK, HP$ at any given time t
PC_{PE}^{CO2}	Penalty cost for CO$_2$ emissions ($/ton)
PC_t^{LOAD}	Cooling load at any given time t
$PE_t^{BESS.M}$	Discharging power from BESS at any given time t
$PE_t^{BESS.P}$	Charging power to BESS at any given time t
PE_t^{BESS}	Power to BESS at any given time t
PE_t^{ELE}	Power to ELE at any given time t
PE_t^{FC}	Power from FC at any given time t
PE_t^{GRID}	Power from grid at any given time t
PE_t^{HP}	Power to HP at any given time t
PE_t^{LOAD}	Electrical load at any given time t (MWh)
PE_t^{PV}	Solar power (MWh) at any given time t
PE_t^{WT}	Wind power (MWh) at any given time t
SOC_t, SOH_t	State of charge of BESS and hydrogen tank at any given time t
u_t^1, u_t^2	Binary variables for on/off of battery

Author contributions

Haider Niaz: Conceptualization, Methodology, Software, Formal analysis, Data curation, Visualization, Writing – original draft, Writing – review & editing. **Mohammad H. Shams:** Writing – review & editing. **Fengqi You:** Writing – review & editing, and Supervision. **Jay. J Liu:** Writing – review & editing, Supervision, Funding acquisition.

Declaration of Competing Interests

The authors declare no competing interests.

Supplementary information

Please find supplementary files with the attachment.

Acknowledgments

Notes and references

1   Cryptocurrency Mining Blamed For Electricity Outages in Iran | Iran International, https://old.iranintl.com/en/iran/cryptocurrency-mining-blamed-electricity-outages-iran, (accessed November 2, 2021).

2   Cambridge Bitcoin Electricity Consumption Index (CBECI), https://cbeci.org/index, (accessed November 1, 2021).

3   World Power consumption | Electricity consumption | Enerdata, https://yearbook.enerdata.net/electricity/electricity-domestic-consumption-data.html, (accessed November 2, 2021).

4   Bitcoin Energy Consumption Index - Digiconomist, https://digiconomist.net/bitcoin-energy-consumption/, (accessed November 11, 2021).

5   K. B. Tokarska and N. P. Gillett, *Nature Climate Change*, 2018, 8, 296–299.

6   Bitcoin mining: Which states are most popular?, https://www.cnbc.com/2021/10/09/war-to-attract-bitcoin-miners-pits-texas-against-new-york-kentucky.html, (accessed November 12, 2021).

7   G. Perboli, S. Musso and M. Rosano, *IEEE Access*, 2018, **6**, 62018–62028.

8   M. Saad, Z. Qin, K. Ren, D. H. Nyang and D. Mohaisen, *IEEE Transactions on Parallel and Distributed Systems*, 2021, **32**, 1961–1973.

9   M. Haouari, M. Mhiri, M. El-Masri and K. Al-Yafi, *Information Processing & Management*, 2022, **59**, 102749.

10   Proof-of-Work vs. Proof-of-Stake: Which Is Better?, https://blockworks.co/proof-of-work-vs-proof-of-stake-whats-the-difference/, (accessed May 31, 2022).

11   Proof of Stake Vs. Proof of Work: What's the Difference?, https://www.businessinsider.com/personal-finance/proof-of-stake-vs-proof-of-work, (accessed May 31, 2022).

12   S. Jiang, Y. Li, Q. Lu, Y. Hong, D. Guan, Y. Xiong and S. Wang, *Nature Communications 2021 12:1*, 2021, **12**, 1–10.

13   C. Stoll, L. Klaaßen and U. Gallersdörfer, *Joule*, 2019, **3**, 1647–1661.

14   H. Niaz, M. M. Lakouraj and J. Liu, *Korean Journal of Chemical Engineering*, 2021, **38**, 1–17.

15   S. L. Náñez Alonso, J. Jorge-vázquez, M. Á. Echarte Fernández and R. F. Reier Forradellas, *Energies (Basel)*, , DOI:10.3390/en14144254.

16   How Texas's wind boom has spawned a Bitcoin mining rush | MIT Technology Review, https://www.technologyreview.com/2020/02/27/905626/how-texass-wind-boom-has-spawned-a-bitcoin-mining-rush/, (accessed November 4, 2021).

17   Rockdale: The Tiny Texas Town That's Turning To Bitmining | TPR, https://www.tpr.org/technology-entrepreneurship/2018-10-15/rockdale-the-tiny-texas-town-thats-turning-to-bitmining, (accessed November 4, 2021).

18   Northern Data Acquires Bitcoin Miner Bitfield N.V. to Become a Leading Global Bitcoin Mining Company with Some 33,000 Latest-Generation ASIC Miners - Northern Data AG, https://northerndata.de/news/northern-data-acquires-bitcoin-miner-bitfield-n-v-to-become-a-leading-global-bitcoin-mining-company-with-some-33000-latest-generation-asic-miners/, (accessed November 5, 2021).

19   Square will invest $5 million to build solar-powered bitcoin mining facility - The Verge, https://www.theverge.com/2021/6/5/22520436/square-invest-5-million-solar-powered-bitcoin-mining-facility-blockstream-cryptocurrency, (accessed November 5, 2021).

20   C. L. Bastian-Pinto, F. V. de S. Araujo, L. E. Brandão and L. L. Gomes, *Renewable and Sustainable Energy Reviews*, 2021, **138**, 110520.

21   M. Andoni, V. Robu, D. Flynn, S. Abram, D. Geach, D. Jenkins, P. McCallum and A. Peacock, *Renewable and Sustainable Energy Reviews*, 2019, **100**, 143–174.

22   California ISO - Managing Oversupply, http://www.caiso.com/informed/Pages/ManagingOversupply.aspx, (accessed April 18, 2021).

23   A. de Vries, *Joule*, 2021, **5**, 509–513.

24   C. Mora, R. L. Rollins, K. Taladay, M. B. Kantar, M. K. Chock, M. Shimada and E. C. Franklin, *Nature Climate Change 2018 8:11*, 2018, **8**, 931–933.

25   L. Dittmar and A. Praktiknjo, *Nature Climate Change 2019 9:9*, 2019, **9**, 656–657.

26   A. de Vries and C. Stoll, *Resources, Conservation and Recycling*, 2021, **175**, 105901.

27   S. Deutz and A. Bardow, *Nature Energy 2021 6:2*, 2021, **6**, 203–213.

28　S. F. Leung, H. C. Fu, M. Zhang, A. H. Hassan, T. Jiang, K. N. Salama, Z. L. Wang and J. H. He, *Energy & Environmental Science*, 2020, **13**, 1300–1308.

29　M. Fasihi, O. Efimova and C. Breyer, *Journal of Cleaner Production*, 2019, **224**, 957–980.

30　M. Pérez-Fortes, J. C. Schöneberger, A. Boulamanti and E. Tzimas, *Applied Energy*, 2016, **161**, 718–732.

31　S. Schlömer, T. Bruckner, L. Fulton, E. Hertwich Austria, A. U. McKinnon, D. Perczyk, J. Roy, R. Schaeffer, G. Hänsel, D. de Jager, T. Bruckner, L. Fulton, E. Hertwich, A. McKinnon, D. Perczyk, J. Roy, R. Schaeffer, R. Sims, P. Smith, R. Wiser, R. Pichs-Madruga, Y. Sokona, E. Farahani, S. Kadner, K. Seyboth, A. Adler, I. Baum, S. Brunner, P. Eickemeier, B. Kriemann, J. Savolainen, S. Schlömer, C. von Stechow, T. Zwickel and J. Minx, *Technology-specific Cost and Performance Parameters*, 2014.

32　J. Nyári, M. Magdeldin, M. Larmi, M. Järvinen and A. Santasalo-Aarnio, *Journal of CO2 Utilization*, 2020, **39**, 101166.

33　Frequently Asked Questions (FAQs) - U.S. Energy Information Administration (EIA), https://www.eia.gov/tools/faqs/faq.php?id=74&t=11, (accessed April 12, 2022).

34　Carbon Dioxide Emissions From Electricity - World Nuclear Association, https://www.world-nuclear.org/information-library/energy-and-the-environment/carbon-dioxide-emissions-from-electricity.aspx, (accessed April 12, 2022).

35　GAMS - Cutting Edge Modeling, https://www.gams.com/, (accessed December 9, 2020).

36　M. H. Shams, M. Shahabi, M. MansourLakouraj, M. Shafie-khah and J. P. S. Catalão, *Energy*, 2021, **222**, 119894.

37　M. H. Shams, M. Shahabi, M. Kia, A. Heidari, M. Lotfi, M. Shafie-khah and J. P. S. Catalão, *Energy*, 2019, **187**, 115949.

38　S. Kwon, W. Won and J. Kim, *Renewable Energy*, 2016, **97**, 177–188.

39　Z. Shi, H. Liang, S. Huang and V. Dinavahi, *IEEE Transactions on Smart Grid*, 2019, **10**, 2234–2244.

40　J. Freeman, N. Blair, D. Guittet, M. Boyd, B. Mirletz, M. Prilliman, T. Neises, M. Wagner, S. Janzou and P.

Gilman, System Advisor Model (SAM), (accessed July 20, 2020).

41　Weather Data & Weather API | Visual Crossing, https://www.visualcrossing.com/, (accessed October 27, 2021).

42　EIA: U.S. Energy Information Administration.

43　Emissions & Generation Resource Integrated Database (eGRID) | US EPA, https://www.epa.gov/egrid, (accessed October 27, 2021).

44　Realtime mining hardware profitability | ASIC Miner Value, https://www.asicminervalue.com/, (accessed October 28, 2021).

45　Bitcoin Mining Calculator - BTC Mining Calculator - CoinWarz, https://www.coinwarz.com/mining/bitcoin/calculator, (accessed March 23, 2022).

46　Bitcoin Price, https://www.coindesk.com/price/bitcoin/, (accessed March 31, 2022).

47　M. Silvia and M. S. Enachescu, *Closed Loop Cryptocurrency Mining in Alberta*, 2019.

48　M. Silvia, *Closed Loop Cryptocurrency Mining in Alberta*, 2019.

49　K. N. Nwaigwe, P. Mutabilwa and E. Dintwa, *Materials Science for Energy Technologies*, 2019, **2**, 629–633.

50　A. Khan, S. Memon and T. P. Sattar, *IEEE Access*, 2018, **6**, 26404–26415.

51　M. H. Shams, H. Niaz and J. J. Liu, *Journal of Power Sources*, 2022, **533**, 231400.

52　A. Mayyas, M. Ruth, B. Pivovar, G. Bender and K. Wipke, *Manufacturing Cost Analysis for Proton Exchange Membrane Water Electrolyzers*, 2019.

53　Depreciation Calculator, https://www.calculator.net/depreciation-calculator, (accessed March 23, 2022).

54　A. Razmjoo, L. Gakenia Kaigutha, M. A. Vaziri Rad, M. Marzband, A. Davarpanah and M. Denai, *Renewable Energy*, 2021, **164**, 46–57.

55　H. Kim, M. Byun, B. Lee and H. Lim, *Energy Conversion and Management*, 2022, **252**, 115119.

56   R. Dickson, E. Mancini, N. Garg, J. M. Woodley, K. v Gernaey, M. Pinelo, J. Liu and S. S. Mansouri, *This journal is Cite this: Energy Environ. Sci*, 2021, **14**, 3542.

57   H. Niaz, M. H. Shams, M. Zarei and J. J. Liu, *Journal of Power Sources*, 2022, **540**, 231558.

58   Proposed U.S. carbon capture credit hike cheers industry, worries greens | Reuters, https://www.reuters.com/world/us/proposed-us-carbon-capture-credit-hike-cheers-industry-worries-greens-2021-11-01/, (accessed April 1, 2022).

59   NATCARB Viewer 2.0, https://edx.netl.doe.gov/geocube/#natcarbviewer, (accessed March 23, 2022).

60   E. Smith, J. Morris, H. Kheshgi, G. Teletzke, H. Herzog and S. Paltsev, *International Journal of Greenhouse Gas Control*, 2021, **109**, 103367.

61   H. Miland and Ø. Ulleberg, 2012, **86**, 666–680.

62   P. Gabrielli, M. Gazzani and M. Mazzotti, *Industrial & Engineering Chemistry Research*, 2020, **59**, 7033–7045.

63   Bitcoin price rises after Elon Musk tweet on energy use, https://www.cnbc.com/2021/05/24/bitcoin-price-soars-after-elon-musk-tweet-on-sustainability-efforts.html, (accessed April 19, 2022).

64   P. Ciaian, M. Rajcaniova and d'Artis Kancs, *Applied Economics*, 2016, **48**, 1799–1815.

65   S. J. H. Shahzad, M. Anas and E. Bouri, *Finance Research Letters*, , DOI:10.1016/J.FRL.2022.102695.

66   T. Tang and Y. Wang, *Journal of Multinational Financial Management*, 2022, 100729.

67   M. S. Akhtar, R. Dickson, H. Niaz, D. W. Hwang and J. Jay Liu, *Green Chemistry*, 2021, **23**, 9625–9639.

68   Bitcoin Electronic Waste Monitor - Digiconomist, https://digiconomist.net/bitcoin-electronic-waste-monitor/, (accessed April 2, 2022).

69   M. S. Akhtar, R. Dickson, H. Niaz, D. W. Hwang and J. Jay Liu, *Green Chemistry*, 2021, **23**, 9625–9639.

70   M. S. Akhtar, R. Dickson and J. J. Liu, *ACS Sustainable Chemistry and Engineering*, 2021, **9**, 17152–17163.

71   M. A. Qyyum, R. Dickson, S. F. Ali Shah, H. Niaz, A. Khan, J. J. Liu and M. Lee, *Renewable and Sustainable Energy Reviews*, 2021, **145**, 110843.

72   M. Ozkan, S. P. Nayak, A. D. Ruiz and W. Jiang, *iScience*, 2022, **25**, 103990.

This journal is © The Royal Society of Chemistry 20xx

Energy Environ. Sci. 2021, **00**, 1-3 | **21**